ISTANBUL TECHNICAL UNIVERSITY ★ GRADUATE SCHOOL OF SCIENCE ENGINEERING AND TECHNOLOGY

SEMICONDUCTOR NANOPARTICLES AS HETEROGENEOUS PHOTOINITIATORS FOR CONVENTIONAL AND CONTROLLED RADICAL POLYMERIZATIONS

M.Sc. THESIS

SAJJAD DADASHI SILAB

Department of Chemistry

Chemistry Programme

Thesis Advisor: Prof. Dr. Yusuf YAĞCI

MAY 2015

ISTANBUL TECHNICAL UNIVERSITY ★ GRADUATE SCHOOL OF SCIENCE ENGINEERING AND TECHNOLOGY

SEMICONDUCTOR NANOPARTICLES AS HETEROGENEOUS PHOTOINITIATORS FOR CONVENTIONAL AND CONTROLLED RADICAL POLYMERIZATIONS

M.Sc. THESIS

SAJJAD DADASHI SILAB
(509121026)

Department of Chemistry

Chemistry Programme

Thesis Advisor: Prof. Dr. Yusuf YAĞCI

MAY 2015

İSTANBUL TEKNİK ÜNİVERSİTESİ ★ FEN BİLİMLERİ ENSTİTÜSÜ

KONVANSİYONEL VE KONTROLLÜ RADİKAL POLİMERİZASYONLARI İÇİN YARIİLETKEN NANOPARÇIKLARIN HETEROJEN FOTOBAŞLATICI OLARAK KULLANIMI

YÜKSEK LİSANS TEZİ

SAJJAD DADASHI SILAB
(509121026)

Kimya Anabilim Dalı

Kimya Programı

Tez Danışmanı: Prof. Dr. Yusuf YAĞCI

MAYIS 2015

Sajjad Dadashi Silab, an **M.Sc.** student of ITU **Graduate School of Science and Technology,** student ID **509121026**, successfully defended the **thesis** entitled "**SEMICONDUCTOR NANOPARTICLES AS HETEROGENEOUS PHOTOINITIATORS FOR CONVENTIONAL AND CONTROLLED RADICAL POLYMERIZATIONS**", which he prepared after fulfilling the requirements specified in the associated legislations, before the jury whose signatures are below.

Thesis Advisor :	**Prof. Dr. Yusuf YAĞCI** Istanbul Technical University	.....
Jury Members :	**Prof. Dr. Gürkan HIZAL** Istanbul Technical University	.....
	Assoc. Prof. Dr. Ersin ACAR Boğaziçi University	.....

Date of Submission : 04 May 2015
Date of Defense : 26 May 2015

To my family,

ACKNOWLEDGEMENT

It has been such a great opportunity for me to be working under the supervision of Professor Yusuf Yagci, one of the leading scientists in the field of polymers. He has been always inspiring and considerate for all of us and taught how to deal with research projects, how to be a critical thinker and how to become a prosperous scientist while having a cheerful social life. I consider myself so privileged to have worked with such a terrific mentor.

During my research in the Yagci group, I have been collaborating with many people from various backgrounds, whom I am so grateful to have worked with. I really appreciate the contributions of my co-supervisors, Dr. Mehmet Atilla Tasdelen and Dr. Baris Kiskan, in my achievements. All current and former members of Professor Yagci's group are also appreciated for being so nice to me.

Thank you all very much.

May 2015 Sajjad Dadashi Silab

TABLE OF CONTENTS

Page

ABBREVIATIONS

NPs : Nanoparticles
ZnO : Zinc Oxide
Fe/ZnO : Iron Doped Zinc Oxide
e^- : Electron
h^+ : Hole
CB : Conduction Band
VB : Valence Band
AAm : Acrylamide
MMA : Methyl Methacrylate
TEA : Triethylamine
$Ph_2I^+PF_6^-$: Diphenyliodonium Hexafluorophosphate
PEGDA : Poly(Ethylene Glycol) Diacrylate
ATRP : Atom Transfer Radical Polymerization
PhotoATRP : Photoinitiated Atom Transfer Radical Polymerization
EBiB : Ethyl α-Bromoisobutyrate
PMDETA : *N,N,N′,N″,N″*-Pentamethyldiethylenetriamine
CuBr : Copper (I) Bromide
$Cu^{II}Br_2$: Copper (II) Bromide
PDI : Polydispersity Index
$CDCl_3$: Deuterated Chloroform

LIST OF TABLES

Page

LIST OF FIGURES

Page

SEMICONDUCTOR NANOPARTICLES AS HETEROGENEOUS PHOTOINITIATORS FOR CONVENTIONAL AND CONTROLLED RADICAL POLYMERIZATIONS

SUMMARY

Semiconducting materials have had a great impact in academia and industry. They offer many potential applications in environmental, analytical, and energetic matters. Semiconductors are highly photosensitive and can promote redox reactions by the photogenerated charge carriers. Electron-hole pairs are released from the conduction and valence band of semiconductor, respectively, upon light illumination.

On the other hand in (photo)polymerization techniques there is a growing demand for more convenient and efficient systems so that polymerization can be conducted straightforwardly under facile conditions with low energy consumptions. Accordingly, a lack of control in conventional photopolymerizations entails much work to devolop or adapt controlled polymerization techniques with emerging or existing photocatalytic concepts.

This prompted us to explore and take the advantages of semiconductor zinc oxide nanoparticles in different photopolymerization systems. We designed a set of reactions in conventional and controlled radical photopolymerizations: free radical polymerization and atom transfer radical polymerization. In the free radical technique, polymerizations were investigated in aqueous and organic media, in which oxygen inhibition problem can partially be suppressed in aqueous environment by including redox reactions of oxygen and water molecules in the formation of initiating radicals. Whereas, in organic media, the process was accomplished with the use of co-initiators. Amine and iodonium salt co-initiators were used to realize redox reactions with the photogenerated holes and electrons, respectively, to form initiating radicals and initiate the polymerization. Several control experiments were carried out to have a clear understanding of the proposed initiation mechanism of each individual system.

The heterogeneous nature of the nanoparticles also offers additional advantage of reusability in further reactions. That is nanoparticles were easily separated off the system and reused for several times under the same experimental conditions without any loss of activity. Doping zinc oxide nanopaticles with iron enhanced the photoactivity of the nanopaticles and gave better results in term of high conversion and rapid reaction time.

There has been a growing interest in developing ATRP systems offering higher and eliminating some drawbacks in conventional ATRP that uses copper(I), including low-stability and high loadings of the copper catalyst. In the controlled photoinitiated atom transfer radical polymerization (photo ATRP), the required copper(I) catalyst was achieved by reduction of copper(II) species with the aid of electrons releasing from the semiconductor under light.

Nanoparticles were able to form *in situ* the copper(I) catalyst by reducing initially loaded copper(II) species. Poly(methyl methacrylate)s were obtained in a controlled manner with well-controlled molecular weights and narrow molecular weight distributions employing ethyl α-bromoisobutyrate as the ATRP initiator, copper(II)Br_2/PMDETA (PMDETA: *N,N,N′,N″,N″*-pentamethyldiethylenetriamine)as the catalyst and zinc oxide nanoparticles as the photocatalyst. Kinetics studies showed all the characteristics of living/controlled polymerization with well-agreement of molecular weights with the theoretical values and high chain end fidelity as approved by ^{1}H NMR spectroscopy and chain extension experiments. Additionally the system exhibited temporal control over the polymerization so that the chain growth could be manipulated by simply switching the light source On/Off.

KONVANSİYONEL VE KONTROLLÜ RADİKAL POLİMERİZASYONLARI İÇİN YARIİLETKEN NANOPARÇIKLARIN HETEROJEN FOTOBAŞLATICI OLARAK KULLANIMI

ÖZET

Son zamanlarda nanoboyutta yapılan malzemeler (nanoparçacık), akademik olarak oldukça araştırılmış olup endüstriyel olarak da geniş kullanım alanına sahiptir. Yarıiletken nanoparçacıklar ışığa duyarlı olduklarından dolayı özellikle incelenmiş ve fotokatalizör olarak birçok alanda kullanılmıştır. Titanyum dioksit (TiO_2), çinko oksit (ZnO), kadmiyum oksit (CdS) gibi inorganik yarıiletken nanoparçacıkların fotokatalizör olarak; hidrojen üretimi, güneş panoları, güneş pilleri, biyolojik ve çevresel uygulamalarda kullanılmaktadır. Fotokatalitik sistemlerin çalışma prensibi, nanoparçacıkların ışıkla uyarılarak elektron-boşluk çift salımına dayalıdır. Aydınlatılarak nanoparçacıklardan salınan yük taşıyıcıları (elektron ve boşluk) yardımı ile su moleküllerini parçalayarak hidrojen ve oksijen üretimi gerçekleşmektedir. Çevreye duyarlı "yeşil" yakıtların üretimi açısından, nanoparçacıkların "yeşil yakıt" olarak hidrojen üretiminde kullanımı büyük önem taşımaktadır.

Fotopolimerizasyon yöntemi, uygulama alanlarındaki artış nedeniyle, gerek endüstri gerekse akademik çalışmalarda gittikçe artan bir öneme sahip olmaktadır. Fotopolimerizasyon, termal polimerizasyona göre düşük enerji tüketimi, oda sıcaklığında sertleşme, çözücüsüz ortamda polimerleşme, uygulanacak yüzey alanı ve uygulama süresinin kontrol edilebilmesi gibi yönleriyle birçok üstün özellik gösterir. Bu özellikler, fotobaşlatılmış serbest radikal polimerizasyonunun çeşitli malzemeler üzerindeki kaplamanın kürlenmesi, diş hekimliği, yapıştırıcılar, matbaa mürekkepleri, kontakt lens ve fotorezistler gibi birçok uygulama için ticari ölçekte yaygın olarak kullanımına imkân sağlar.

Günümüzde fotobaşlatıcılarla ilgili yapılan araştırmaların büyük bir bölümü, yeni başlatıcıların sentezi veya mevcut başlatıcıların çözünürlüklerini geliştirme amacı taşımaktadır. Fotokimyasal yolla başlatılan radikal polimerizasyon bölünme (*Tip I*) ve hidrojen-koparma tipi (*Tip II*) fotobaşlatıcılar tarafından başlatılır. Fotopolimerizasyonda, fotobaşlatıcıların büyük öneme sahip olması nedeniyle, geniş ölçüde araştırmaya tabidir. Birinci tip fotobaşlatıcılar, aydınlatma sonucu α-bölünme süreci ile iki tür radikal vermek üzere fotoparçalanmaya uğrarlar. *Tip II* fotobaşlatıcılar, aydınlatma sonucu triplet uyarılmış hal α-hidrojen verici bileşiklerle reaksiyona girerek başlatıcı radikali oluşturur. Genellikle mor ötesi veya görünür bölge ışık kaynakları kullanılır. Fotobaşlatıcının uygun bir dalga boyundaki ışık absorpsiyonu sonucunda oluşan primer radikaller tek fonksiyonlu monomerlerin polimerizasyonunu sağlarken çok fonksiyonlu monomerlerin de çapraz bağlı yapılara dönüştürülmesini sağlar.

Bütün üstünlüklere rağmen, fotopolimerizasyonda kullanılan düşük molekül ağırlıklı fotobaşlatıcılarla ilgili bazı dezavantajlar ortaya çıkmaktadır. Örneğin, kürlenmiş

filmlerde fotobaşlatıcının parçalanmasından ortaya çıkan yan ürünler zamanla yüzeye göçerek filmi kullanılamaz hale dönüştürür. Bu dezavantajları ortadan kaldırmak için bir takım yöntemler geliştirilmiştir. Makrofotobaşlatıcılar (polimerik fotobaşlatıcılar) kullanarak filmlerde göçme dezavantajı ortadan kaldırılmaya çalışılmıştır. İkinci tip fotobaşlatıcı sistemlerde ise kullanılan hidrojen verici grubu ve fotobaşlatıcıyı birleştirmesi ile tek-bileşen fotobaşlatıcı sentezleyerek, hidrojen verici gruplardan ortaya çıkan zehirli ve kötü koku giderilmiş oluyor.

Bu tezde, yukarıda belirtilen fotopolimerizasyondaki olumsuzlukları ortadan kaldırmak için çinko oksit (ZnO) nanoparçacıkları üretimi ve heterojen fotobaşlatıcı kullanımına dayalı iki farklı strateji ortaya konmuştur.

İlk strateji, ışığa duyarlı çinko oksit nanoparçacıkların fotopolimerizasyonda başlatıcı olarak kullanımı üzerine kurulmuştur. Çinko oksit nanoparçacıkları tarafından ışıkla uyarıldıklarında ortama elektron-boşluk yük taşıyıcı çiftleri salınır. Ortamda bulunan elektron-boşluk çiftleri ile redoks reaksiyonlarına uygun eş-başlatıcı (co-initiator) molekülleri üzerinden serbest radikaller oluşur ve ardından vinil monomerlerin polimerizasyonu başlatılır. Serbest radikal polimerizasyonu, çinko oksit nanoparçacıkları kullanılarak sulu ve organik ortamda incelenmiştir. Sulu ortamda okijen ve su molekülleri üzerinden yürüyen redoks reaksiyonları sonucunda oluşan hidroksil radikali akrilamit polimerizasyonunu başlatır. Farklı koşullarda yapılan kontrol deneyleri yapılarak başlatma mekanizması aydınlatılmıştır. Böylelikle yarıiletken nanoparçacıkları kullanılarak ortamdaki oksijen moleküllerini başlama mekanizmasında tüketerek polimerizasyonda oksijen bulunma problemi de ortadan kalkmış olur.

Organik ortamda ise metil metakrilat polimerizasyonu iki farklı eş-başlatıcı türü varlığında yapıldı. Bunun için, fotopolimerizasyonda en yaygın kullanılan amin ve onyum tuzları eş-başlatıcı olarak kullanıldı. Fotopolimerizasyonda amin eş-başlatıcıları uyarılmış triplet hal fotobaşlatıcılarını indirgeyerek radikal türleri üretirler. Onyum tuzları ise uyarılmış triplet hal fotobaşlatıcılardan bir elektron alarak, fotobaşlatıcıyı yükseltip serbest radikal türlerini oluşturur. Bu çalışmada kullanılan trietil amin eş-başlatıcısı nanoparçacıklardan ışık altında oluşan boşlukla etkileşime girerek yükseltgenip ardından başka bir amin molekülünden hidrojen koparak serbest radikaller oluşturur. Onyum tuzu varlığında ise çinko oksit nanoparçacıklarından ışık altında salınan elektronlarla bir indirgeme reaksiyonu gerçekleşir. Difeniliyodonyum tuzu bir elektron alarak difenil iyodür radikaline dönüşür. Ardından, oluşan bu radikal fenil iyodür ve fenil radikal türlerine parçalanır. Trietil amin ve difeniliyodonyum eş-başlatıcılarından redoks reaksiyonları sonucunda oluşan α-amino radikal ve fenil radikal türleri metil metakrilat gibi vinil tip monomerlerin polimerizasyonunu başlatır.

Bütün bu reaksiyonlar organik ortamda yapılırken, suda çözünen monomerlerin polimerizasyonu da çinko oksit nanoparçacıkları kullanılarak gerçekleşir. Suda çözünen monomer olarak akrilamit monomeri kullanıldı. Sulu ortamda ve oksijen varlığında başlatma mekanizması hidroksil radikallerin oluşumu ile gerçekleşti. Kontrol deneyleri yapılarak hidroksil radikallerin oluşumu izlendi. Işık altında nanoparçacıklardan oluşan boşluklar su molekülleri ile reaksiyon verip hidroksil radikali oluşturur. Oksijen molekülleri ise elektron alarak oksijen radikal anyonu oluşturur ve ardından oluşan bu radikal anyon su molekülleri ile reaksiyona girerek hidroksil radikali oluşturur. Böylelikle oksijen molekülleri serbest radikal

oluşumunda kullanılarak, polimerizasyonda serbest radikallerin oksijen ile sonlandırma problemi büyük ölçüde ortadan kalkmış olur.

Yarıiletken nanoparçacıkların foto-aktivitesini arttırmak için kullanılan yöntemlerden birisi doplama yöntemidir. Doplama için kullanılan elementler nanoparçacıkların kristal yapısında safsızlık olarak ışıma altında yük taşıyıcıların salınımını kolaylaştırır. Bu çalışmada ise demirle doplanmış çinko oksit nanoparçacıkları sentezlenip fotopolimerizasyon reaksiyonlarında kullanıldı. Doplanmış nanoparçacıklarla yapılan deneylerde, polimerizasyon hızında ve monomer dönüşümünde bir artış izlendi.

Tezin ikinci kısmında çinko oksit nanoparçacıkların kontrollü/yaşayan polimerizasyon türü olan atom transfer radikal polimerizasyonunda (ATRP) kullanımını incelemek amacı ile yapılmıştır. Fotokimyasal olarak başlatılan kontrollü/yaşayan polimerizasyonlarda zincir transfer ve depolimerizasyon gibi yan reaksiyonların minimize edilmesinden dolayı daha düşük molekül ağırlık dağılımına sahip polimerler elde edilmektedir. Ayrıca uygun fotobaşlatıcı ve ışık şiddeti seçilerek de hem başlatıcı konsantrasyonu hem de polimer zincirlerinin boyu ayarlanabilir. Günümüzde var olan foto-ATRP sistemlerinde bakır(II) iyonları farklı fotokimyasal yöntemleri ile bakır(I)'e indirgeyerek ATRP için gerekli olan bakır(I) katalizörü elde edilir.

Tez çalışmalarının bu kısmında ise çinko oksit ve demir doplu çinko oksit nanoparçacıkları yardımı ile fotokimyasal olarak ATRP için bakır(I) katalizörü üretimi incelenmiştir. Bunun için metil metakrilat, alkil halojenür, bakır(II) bromür ve çinko oksit nanoparçacıkları varlığında ışık altında denemeler yapılmış ve elde edilen polimerlerin molekül ağırlığı ve dağılımı, ve birçok parametrenin polimerizasyon üzerine etkisi incelenmiştir. Elde edilen sonuçlar ışığında sistem için monomer tüketimi/zaman ve molekül ağırlığı/dönüşüm grafikleri çizilip, sistemlerle ilgili kinetik çalışmaları yapılmıştır.

1. INTRODUCTION

Nanoscale materials have been the center of contemporary researches in many interdisciplinary areas. Semiconductor nanoparticles (NPs) often referred to as quantum dots (QDs), have been investigated in many catalytic purposes. Owing to their photosensitive properties, semiconducting materials have been extensively utilized as photocatalyst, which can be excited upon irradiation and provide the required charge carriers to induce reactions by enabling reduction/oxidation processes [1]. Numerous photocatalytic applications have been carried out employing semiconductor NPs as the photocatalyst. Examples include water splitting to evolve hydrogen [2], biosensing [3], sensitizers in solar cells [4], remediation of pollutants and water purification [5, 6], and many other photocatalytic processes [7, 8]. The photocatalytic activity is based on the excitation of semiconductor NPs under light and consequent formation of electron-hole pair.

There has been an intense research interest towards light-induced polymerization techniques by which polymers could be achieved upon absorption of energy by light sensitive species and providing active initiating sites to initiate polymerization. In addition to conventional radical polymerization, controlled/living polymerization techniques such as atom transfer radical polymerization (ATRP) or reversible addition–fragmentation chain transfer (RAFT), in particular, have drawn much more attention towards light-driven processes due to the ability of producing well-defined and complex macromolecular structures by these techniques and ease of achieving these with light-induced processes.

Merging these two research areas of semiconducting photocatalysis and photopolymerization would open new avenues in synthetic polymer chemistry.

2. THEORETICAL PART

2.1 Heterogeneous Photocatalysis

Concerns about durability of fossil fuels and their destroying effects on environment has grown attention to more abundant and green forms of energy such as solar energy to use in many chemical reactions and even in our daily life. Photochemistry of homogeneous metal-complexes and heterogeneous semiconductor naomaterials has been exploited to converting light into chemical energy. A striking example of this is splitting of water into hydrogen and oxygen, the so-called the “holy grail” of photochemistry. The overall mechanism of photocatalytic process is depicted in Figure 2.1.

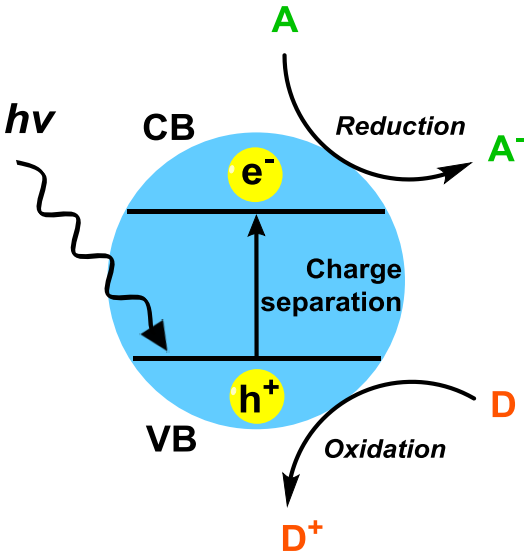

Figure 2.1 : Overall photoexcitation mechanism and subsequent redox reactions by the charge carriers from semiconducting materials.

2.2 Photoinitiated Polymerization

2.2.1 Photoinitiated free radical polymerization

Photoinitiated polymerization is one of the most versatile and efficient techniques in polymer community. The use of light as driving force to initiate the process has made it possible to reduce the fabrication process cost and to suppress some drawbacks

rising in thermal processes under milder conditions [9]. It has been applied in various applications including coatings, adhesives, inks, printing plates, optical waveguides, microelectronics, dental fillings and fabrication of 3D objects etc. The role of light in such systems is mainly confined to the very first step of the reaction that is to form active initiating species such as free radicals or cations to initiate polymerization. Photoinitiators, therefore, play a major role in photopolymerization. They are generally classified into two classes of *Type I* (also known as α-cleavage) and *Type II* (hydrogen abstraction type). Disassociation of *Type I* photoinitiators upon absorption of light directly gives rise to the initiating radicals, while in *Type II* systems abstraction of a hydrogen by photoexcited (triplet state) photoinitiator encounters for the formation of radicals.

There have been reported some disadvantages regarding the use of low-molecular weight photoinitiators such as migration from cured films or strong odor sprung mostly from co-initiators. A practical way to overcome these disadvantages is to use macromolecular/heterogeneous photoinitiators or designing one-component photoinitiators to eliminate the use of co-initiators.

With regard to heterogeneous photoinitiators, mesoporous graphitic carbon nitride (mpg-C_3N_4) was reported as an efficient heterogeneous photocatalyst working in the visible range of magnetic spectrum for photoinitiated free radical polymerization [10].

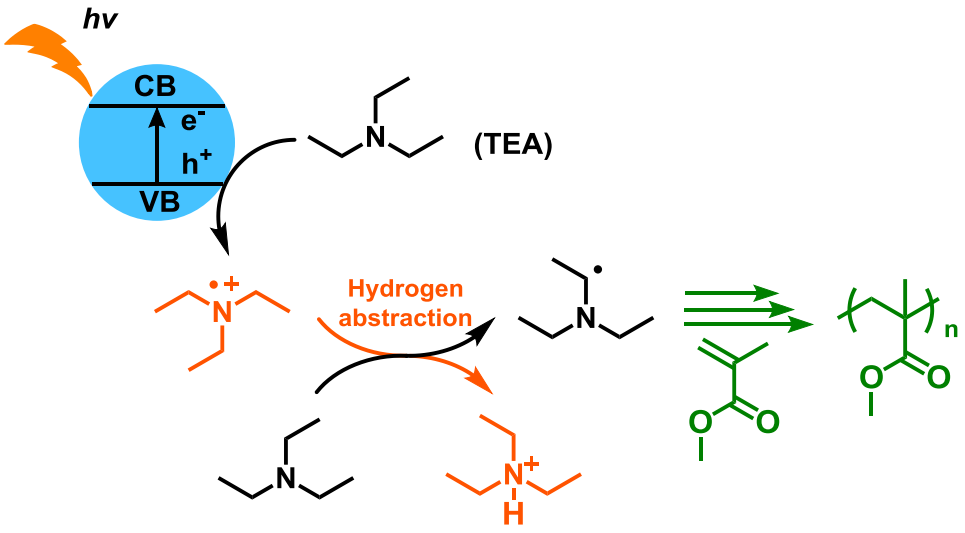

Figure 2.2 : Initiation mechanism of the free radical polymerization by using mesoporous graphitic carbon nitride in the presence of amines as co-initiators.

It was found that the mesoporous material exhibits excellent performance in the initiation and could easily be separated from the polymerization mixture and reused without any significant loss of the activity. The proposed initiation mechanism of the polymerization using mpg-C_3N_4 is based on the generation of an electron and a hole under the visible light irradiation. Holes can oxidize organic molecules such as amines, alcohols, and vinyl monomers leading to the formation of radicals, which can react further with the monomer and thereby initiate polymerization chains (Figure 2.2).

2.2.2 Photoinitiated controlled radical polymerization

Interest has also grown in photoinitiated-controlled polymerization techniques. Controlled radical polymerizations offer additional advantages of gaining control over the reaction process to implement desired architecture and composition. Otsu and co-workers reported the first example of the photoinitiated-controlled radical polymerization where the initiator-chain transfer-termination (iniferter) concept was used in polymerization of vinyl monomers in the presence of a dithiocarbamate (DTC) as photoiniferter agent under irradiation. The carbon-sulfur bonds present in DTC are readily cleaved upon irradiation, which give active radicals to add double bonds where following deactivation by the sulfur-centered radicals a control can be achieved. This concept further led to the synthesis of photolabile polymer structures [11, 12] or eliminating some drawbacks encountered in both iniferter and ATRP processes when combined [13].

2.2.3 Photoinitiated ATRP

During the past years, for environmental and practical issues, various initiation techniques involving *in-situ* generation of the activator catalyst have been reported to accomplish ATRP in more pragmatic condition i.e., in the presence of oxygen, at room temperature or the use of catalyst at the level of parts per million (ppm). To date, several approaches have been undertaken to develop ATRP process (Figure 2.3). For instance, reverse ATRP, simultaneous reverse and normal initiated (SR&NI), activators by electron transfer (AGET), activators regenerated by electron transfer (ARGET) [14], initiators for continuous activator regeneration (ICAR) [15, 16], and supplementary activator and reducing agent (SARA) ATRP [17, 18], and single electron transfer-living radical polymerization (SET-LRP) have been reported.

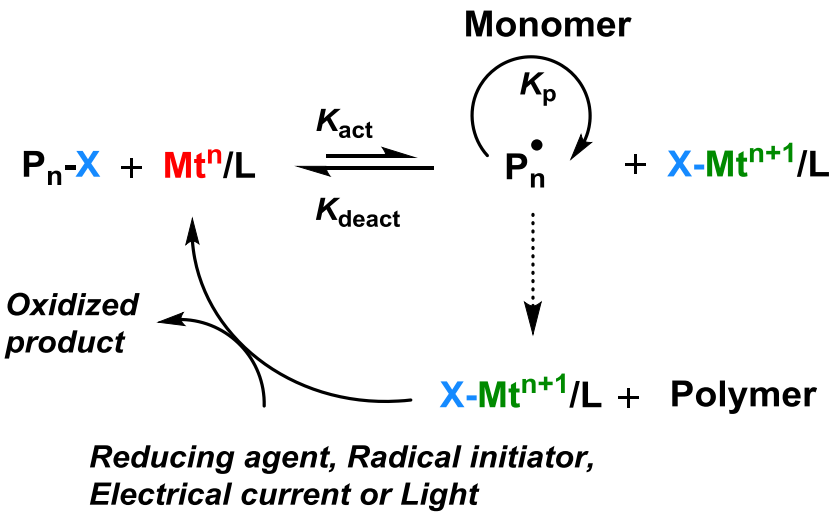

Figure 2.3 : Regeneration of activator via electron transfer mechanisms using various reducing methodologies.

These methods benefit from different reduction processes to the *in-situ* formation of activator Mt^n including (I) use of various reducing agents [19], (II) electrochemically redox processes [20], (III) copper-containing nanoparticles [21], and (IV) photochemically mediated redox processes [22-26].

Overall, recently developed initiating systems eliminate the problem with high catalyst concentration and catalyst oxidation and make a huge step towards making ATRP an industrially viable process (Figure 2.4). The polymerization reaction can be stopped and restarted simply by switching light or electric current on and off.

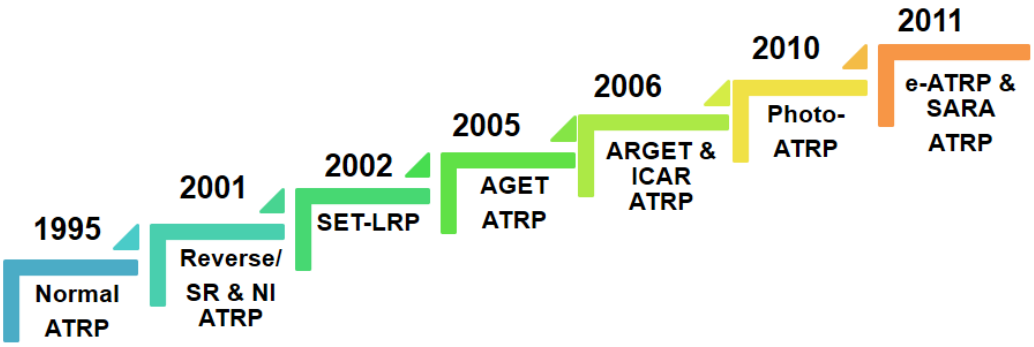

Figure 2.4 : Chronological development of initiating systems for ATRP.

Light is a widely available, non-invasive, and environmentally benign reagent that provides opportunities for both spatial and temporal control of ATRP process [9, 27]. Since Cu(II) species are photochemically reduced in the presence of amine ligands, Yagci and coworkers used this reaction to generate active Cu(I) species from air stable Cu(II) species. The mechanism is similar to AGET or ARGET ATRP, though

a stoichiometric or substoichiometric Cu(II) catalyst over an ATRP initiator was employed. Various photoactive molecules including commercial photoinitiators or dyes are also effective reducing agents of Cu(II) and facilitate the photoinitated ATRP process.

In 2000, Guan and Smart reported the photo-enhanced ATRP of methyl methacrylate (MMA) by visible light irradiation [28]. They observed considerable enhancement in the rate of polymerization under visible light irradiation as compared to the dark conditions. Polymerization of MMA (with [MMA]/[RCl]/[CuCl]/[bipy] : 100/0.1/0.3/1 ratio), reached to 41% of monomer conversion after 16 h at 80 °C in the dark, whereas employing visible light to the same conditions gave 100% of monomer conversion having molecular weights near to the theoretical values with narrow molecular weight distributions. Though the exact effect of the light was not clear, they attributed it to the acceleration of the activation of the inner-sphere complex between the catalyst and the alkyl chloride, [Cu(I), R-Cl], or through the activation of the catalyst alone by light.

2.2.3.1 Directly generated activator for photoinitiated ATRP

Many copper(II)/ligand complexes are known to be light sensitive and undergo photoredox reactions during UV-irradiation [29, 30]. Moreover, the polymerization of various vinyl monomers can be initiated by the photoproducts of Cu(II)/L complexes in both aqueous and organic media [31, 32]. Previous spectroscopic studies pointed out that Cu(II) complex has three distinct absorption bands at 250, 300 and 640 nm [33, 34]. Under UV irradiation of monomer mixture containing ethyl 2-bromopropionate (EtBP)as alkyl halide, $Cu^{II}Br_2$/PMDETA as catalyst and MMA as monomer, Cu(II) d-d ligand field transition band centered at 640 nm diminishes and gives rise to the lower energy shoulder (Figure 2.5). However, the formation of Cu(I) cannot be monitored because of overlapping with the characteristic peak of Cu(II) complex at 300 nm [35]. The strong absorption at this wavelength corresponding to the ligand-to-metal charge-transfer transition is responsible for the photoreduction of Cu(II) to Cu(I) [36].

Polymerization of MMA was accomplished by reduction of Cu(II) to Cu(I) upon absorption of light and subsequent activation of alkyl halide [23]. A linear relationship was observed between the monomer consumption and polymerization

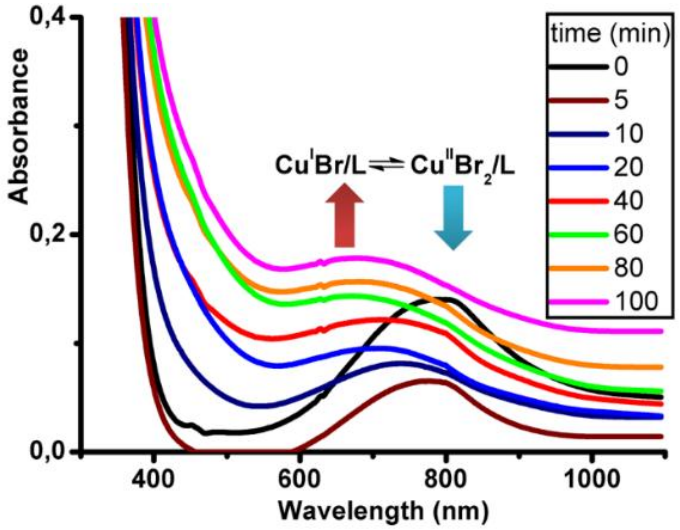

Figure 2.5 : Typical UV/Vis spectral changes of the initiating system by UV irradiation at 350 nm. UV spectra were recorded after exposing the solution to light for subsequent intervals during 100 min.

time and evolution of molecular weight *vs* conversion revealing of well-controlled process. The molecular weight of the obtained polymers having narrow molecular weight distributions, were in well agreement with the theoretical values. In subsequent work the enhancement of the same process by adding of small amount of methanol was reported [22]. The use of small amount of methanol as solvent in the polymerization facilitated to conduct the process in homogeneous system, as methanol exclusively penetrates the solubility of Cu(II) complexes in the polymerization mixture. By applying homogenous polymerization of MMA, the rate of polymerization increased significantly when compared with the heterogeneous system, and the control over molecular weights under homogenous system was improved. In both works, the livingness of the obtained polymers was confirmed by chain extension experiments. The amount of Cu(II) catalyst used in these studies was in equivalent with respect to initiator.

Later on, Mosnacek and Ilcikova applied Cu(II) catalyst at the ppm level of 50-100 to conduct photochemically mediated ATRP of MMA under UV light irradiation [37]. The use of 100 ppm of $Cu^{II}Br_2$/PMDETA catalyst (0.02 equivalents with respect to initiator) in 25 vol% of anisole as a solvent proceeded the polymerization in well controlled manner giving PMMA with molecular weight close to the theoretical value and with narrow distributions. The rate of polymerization as well as the level of control were very similar to ARGET ATRP using tin(II) octanoate as a reducing agent. The catalyst loading could be further reduced to 50 ppm by using

tris(2-pyridylmethyl)amine (TPMA) as a ligand with maintaining a high level of control, but further reduction of the Cu catalyst to 25 ppm resulted in a loss of control. The higher efficiency of the TPMA ligand over PMDETA was attributed to the higher stability of the Cu(II) complex of the former ligand than that of the latter.

Recently Matyjaszewski et al. reported the use of visible light and sunlight for photoinduced ATRP with ppm of Cu catalyst without use of any photoinitiator or reducing agent [26]. In their proposed mechanism, photoexcited Cu^{II}/L reduced to Cu^{I}/L directly, which was used as activator in the ATRP. Subsequently, polymerization was started by the activation of an R-X initiator by the Cu^{I}/L activator. Notably, a halogen radical ($X^{\bullet}$), which is capable of initiating polymerization, was formed. This resembled a hybrid mechanism of ICAR and ARGET ATRP. The process was photochemically directed as evidenced by consecutive light and dark reactions. The polymerizations at 390 nm provided faster polymerization rate and well-controlled results as compared to the 450 nm. Interestingly, irradiations at 632 nm failed to initiate the polymerization indicating inefficiency of the photoactivation at low energy ranges. Additionally, this process was successfully tested for aqueous systems using oligo(ethylene oxide) monomethyl ether methacrylate as monomer and poly(ethylene oxide) monomethyl ether bromoisobutyrate as initiator with molecular weight of 2000 g mol^{-1}, 100 ppm of a $Cu^{II}Br_2$/TPMA catalyst, with 30 mM NaBr in water (67% by volume).

Haddleton and co-workers have recently reported photoinitiated ATRP of acrylates directed by a photoredox process of $Cu^{II}Br_2$ and an aliphatic tertiary amine.[38, 39] Their process is based on the *in-situ* photoreduction of air stable Cu(II) species without using any conventional photoinitiator or photosensitizer under daylight or UV radiation. A variety of vinyl monomers including poly(ethylene glycol) methyl ether acrylate, *tert*-butyl acrylate, methyl acrylate (MA), MMA, and St, as well as functional initiators in different solvents were tested. The polymerization of MA with [MA]/[EBiB]/[Me_6-Tren]/[$Cu^{II}Br_2$] : 50/1/0.12/0.02 ratio in DMSO gave 99% of monomer conversion after 15 h (EBiB: ethyl 2-bromoisobutyrate). Control experiments revealed that the Me_6-Tren ligand must be loaded in excess with respect to Cu(II), as no polymerization took place when the ligand was employed in one equivalent. Increasing the ligand ratio to 2 just started the polymerization while the use of 3 equimolar of Me_6-Tren gave a slightly better result. The process exhibited

all the characteristics of a living process, including a linear relationship between molecular weight and conversion, a good agreement between theoretical and obtained molecular weights, and low molecular weight distribution. The degree of chain end functionality has been exemplified by chain extension and block copolymerization via sequential monomer addition.

Despite all good results for acrylate monomers, the system did not work very well for MMA and St as the molecular weight distributions were 1.29 and 1.40 (conversions 78% and 40%), respectively. The proposed mechanism is based on the absorption of light by free Me_6-Tren ligand, which results the photoexcited [Me_6-Tren]*. Then, outer-sphere single-electron transfer from photoexcited leads to homolysis of C-Br forming a required initiating radical and a Me_6-Tren radical cation with a Br^- counterion. These radicals were not only able to add to monomer molecules to initiate growth of polymer chains but also reduced the $Cu^{II}(Me_6\text{-Tren})Br_2$ to $Cu^{I}(Me_6\text{-Tren})Br$, which was used as activator in the ATRP. Although, the mechanism is complex and highly dependent upon the reaction conditions, including solvent, temperature, and catalyst loading, it provides well-defined poly(acrylates) in excellent conversions, rates, and end group fidelity under UV irradiation.

This process was also applied for the synthesis of sequence-controlled multi-block copolymers. Different acrylate monomers, methyl acrylate, ethyl acrylate, ethylene glycol methyl ether acrylate and solketal acrylate were used to prepare multi-block copolymers, up to a dodeca-block (12 blocks), containing repeat units comprised of four alternating monomer sequences whilst maintaining narrow polydispersities (PDI <1.20) [40] .

The ability of other transition metals such as iridium (Ir), and ruthenium (Ru), as alternative to the cupric catalyst system, were investigated to succeed photoinitiated ATRP. Recently Hawker et. al. investigated the Ir-based photoredox system that can be utilized in order to control the polymerization of methacrylate monomers [41]. The *fac*-[$Ir(ppy)_3$] (ppy =2-pyridylphenyl) was used as the catalyst which affords photoexcited *fac*-[$Ir(ppy)_3$]* species upon irradiation under visible light. The photoexcited Ir^{III}* captured a halogen atom from alkyl halide to form initiating radicals as well as highly oxidized Ir^{IV} complex. This Ir^{IV} could then react with the propagating radical to generate initial Ir^{III} complex in the ground state (Scheme 3). Well-defined PMMAs were obtained using ppm amounts of Ir-based catalyst under

visible light irradiation. However, high catalyst loading, such as 0.5 equivalent over the initiator, resulted in uncontrolled process (M_w/M_n = 2.76) since the Ir catalyst acted only as an initiator in this system. The overall mechanism is depicted in Figure 2.6.

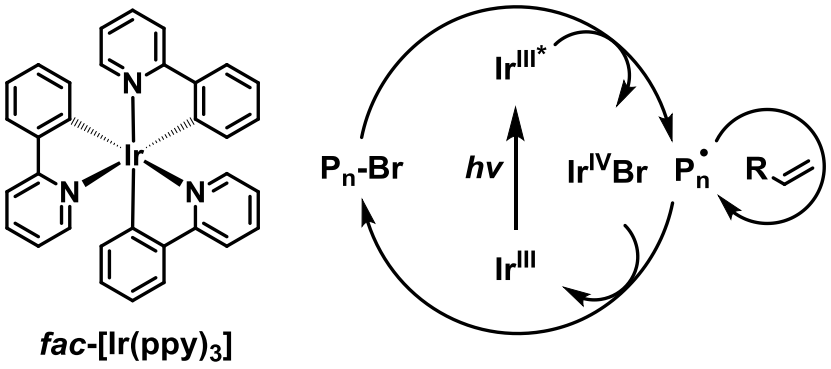

Figure 2.6 : The Ir-based photoredox catalyst system for visible light-mediated ATRP.

The same group also established spatiotemporal control over the patterning of polymer brushes using the same catalytic system under visible light irradiation [42, 43]. For this purpose, alkyl halide functionalized substrates immersed in a solution of MMA and [Ir(ppy)$_3$] in DMF and irradiated directly with visible light. The results showed clear patterning of the PMMA brushes demonstrating spatial control over brush formation from a uniform initiating layer and the ability to pattern a range of features over large areas as shown in Figure 2.7.

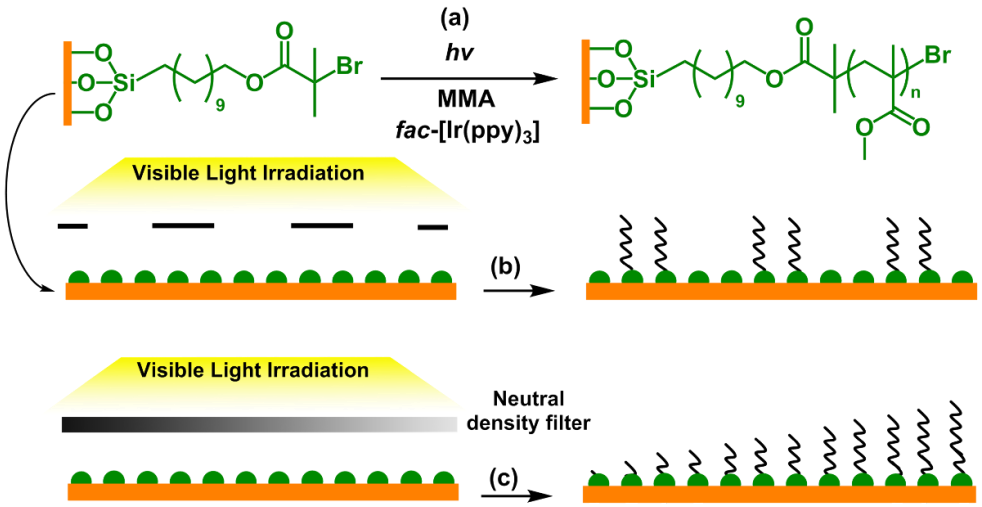

Figure 2.7 : Patterning of polymer brushes from substrates uniformly functionalized with trichlorosilane-substituted ATRP initiators (a) using a photomask for patterns (b) or a neutral density filter (c) for gradient structures.

Additionally neutral density filters could be used to modulate the intensity of incident light as well as the rate of polymerization from the surface. Choosing the correct spatial and temporal patterning parameters can allow the fabrication of three-dimensional nanostructures in a controlled fashion from polymer brushes.

2.2.3.2 Indirectly generated activator for photoinitiated ATRP

Many UV and visible light free radical photoinitiators were reported to be powerful promoters for photoinitiated ATRP. For this purpose, the photoinitiated reverse ATRP in the absence of alkyl halide and photoinitiated SR&NI ATRP in the presence of alkyl halide were extensively investigated using commercially available photoinitiators. Photoinitiated reverse ATRP was performed using the $Cu^{II}Br_2$/PMDETA system in conjunction with several photoinitiators belonging to both *Type I* class, such as 2, 2-dimethoxy-2-phenyl acetophenone, (2,4,6-trimethylbenzoyl) diphenylphosphine oxide (BAPO) [44] and *Type II* class such as benzophenone, at room temperature. Even though the polymerization of MMA could be initiated in the absence of alkyl halide, loss of control over the polymerization process was observed. The type and concentration of photoinitiators directly affect the photoinduced reverse ATRP. Photoinitiated SR&NI ATRP was successfully applied to MMA in the presence of EtBP. The molecular weights increased with conversion, and they were in good agreement with the theoretical values.

Compared to the photoinduced reverse ATRP, it allowed better control over molecular weights with narrow molecular weight distributions. Notably, the chain extension reaction with the macroinitiator prepared by photoinitiated SR&NI ATRP was more successful than photoinitiated reverse ATRP.

Subsequently, the photoinitiated reverse ATRP by employing camphorquinone/benzhydrol (CQ/Bzh) as the initiating system was also developed [45]. Both Bzh and PMDETA ligand could act as the hydrogen donor to form ketyl radicals (inactive towards the monomer) from the photoexcited CQ reducing Cu(II) to Cu(I). However, Bzh gave better results in terms of relatively controlled process. Although the process seemed to be less controlled, as the resulted polymers had broad molecular weight distributions and less agreement with the theoretical values, their living nature was high when SR&NI ATRP was applied in chain extension experiment.

Recently Yagci et al. investigated the photoinitiated ATRP to extend its spectral sensitivity to the visible range by either adding a dye or a visible light photoinitiator [46]. The primary photochemical reaction involves the excited dye molecules abstract an electron from the amine molecules to form radical-cation/radical-anion pairs. After the proton transfer, some of the radicals were in the system. These radicals were not only able to add to monomer molecules to initiate growth of polymer chains but also reduced the $Cu^{II}Cl_2$ to $Cu^{I}Cl$, which was used as activator in the ATRP. Generally, only the radicals generated from the amine component were reactive enough to activate the polymerization. The radicals generated from the dye molecules were believed to act mostly as radical chain terminators or undergo other reactions leading to bleaching the dye. Although, the molecular weights increased with conversion linearly, the experimental molecular weights were considerably higher than theoretical values in the dye-sensitized systems. In addition, the molecular weight distributions were relatively high, ranging from 1.28-1.60 and reasonable control were observed under visible light irradiation. The polymers obtained by *Type I* system, BAPO, had molecular weight values close to the theoretical ones and very narrow molecular weight distributions ranging from 1.11-1.18. Compared to the dye-sensitized SR&NI ATRP, it showed better control of molecular weight and distribution under the same experimental conditions.

The overall mechanism of photoinitiated ATRP using *Type I* or *Type II* photoinitiators as reducing agents is depicted in Figure 2.8.

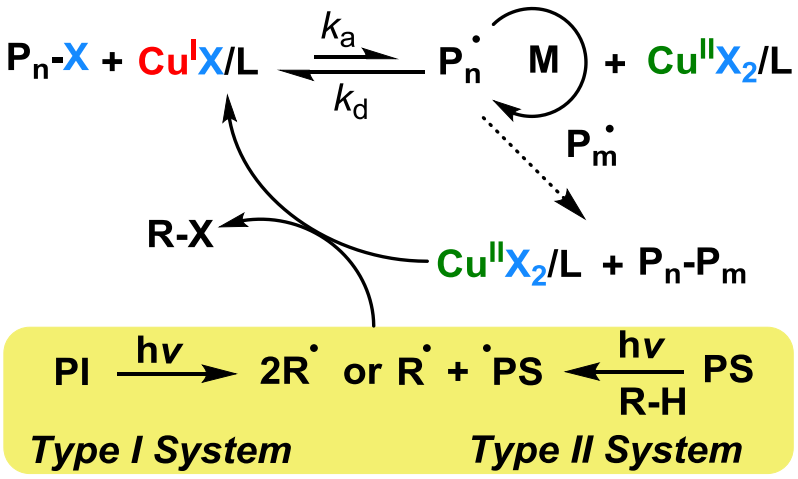

Figure 2.8 : Proposed mechanism for dye-sensitized SR&NI ATRP using *Type I* or *Type II* photoinitiating systems (PI: photoinitiator; PS: photosensitizer and R-H: hydrogen donor).

Another versatile approach for photoinduced ATRP is based on the photolysis of dimanganese decacarbonyl ($Mn_2(CO)_{10}$) under visible light or sunlight illumination.[47] The photoredox behavior of $Mn_2(CO)_{10}$ in the system was followed by means of UV-vis spectra [48-51]. Optical absorption of the polymerization solution ([MMA]/[EtBP]/[$Cu^{II}Br_2$]/[PMDETA]/[$Mn_2(CO)_{10}$]) was found to be decreased upon irradiation, indicating the reaction of $Mn_2(CO)_{10}$ with either P_n–Br or $Cu^{II}Br_2$/PMDETA. Admittedly, appearance of a new peak at 455 nm upon irradiation, when alkyl halide was absent, corresponded to the ligand-to-metal charge-transfer transition of a copper metal. This indicated direct reduction of Cu(II) to Cu(I) by $^{\bullet}Mn(CO)_5$ radicals. The formed radicals were reported to abstract halogen atoms from alkyl halides to generate carbon centered radicals or reducing $Cu^{II}Br_2$ to $Cu^{I}Br$ directly, which was used as an activator in the ATRP of vinyl monomers such as MMA, MA and St. The growth of the polymer chain was manipulated by either varying the $Mn_2(CO)_{10}$ concentration or adjusting the light intensity, which changed the concentration of the Cu(I) catalyst. Moreover, this method was also used to synthesize graft copolymers from commercially available poly(vinyl chloride) (PVC) without additional modification. The chlorine atoms of PVC can act as initiation sites for the direct grafting of MMA by visible light induced ATRP. The molecular weight measurements showed a monomodal molecular weight distribution and a significant shift of the peak value toward higher molecular weights. This confirmed the successful graft copolymerization without detectable free homopolymer formation (Figure 2.9).

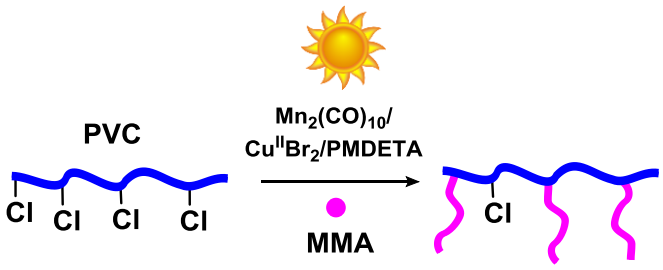

Figure 2.9 : Direct grafting of MMA from PVC via visible light induced ATRP using $Mn_2(CO)_{10}$.

More recently, the photoinitiated ATRP has been implemented in the inverse microemulsion polymerization of oligo(ethylene glycol) monomethyl ether methacrylate. Two different initiation systems including SR&NI ATRP and a combination of AGET and ICAR ATRP were developed under UV light [52]. A

stable and bluish water/oil inverse microemulsion was generated after mixing polymerization solutions (aqueous phase: $Cu^{II}Br_2$, PMDETA or TPMA as a ligand and PEO-Br as a macroinitiator, PEG 550 a co-stabilizer, OEOMA as a monomer and water as solvent; oil phase: a mixture of polyoxyethylene (3) oleyl ether and polyoxyethylene (6) oleyl ether as surfactants and hexane as solvent), forming small aqueous monomer swollen ‘‘micelles’’/droplets with the copper catalyst precursors encapsulated inside. The photoinitiated SR&NI ATRP was initiated by activating the catalysts via UV light irradiation of water-soluble photoinitiator (Irgacure 2959). Whereas AGET&ICAR ATRP system, direct photolysis of Cu(II)/TPMA deactivator complex can also induce a redox reaction of between Cu(II)/TPMA and Cu(I)/TPMA activator plus bromine radical to start the polymerization and then continue to regenerate the activator lost in the biradical termination process. Not only photoinitiated SR&NI ATRP but also photoinitiated AGET & ICAR ATRP produced nanometer-sized particles with narrow and monomodal size distribution. Moreover, the polymers obtained by two systems had molecular weight values close to the theoretical ones and relatively narrow PDI ranging from 1.20-1.40. The method is particularly advantageous for tuning the particle size which, could be manipulated by changing the aqueous phase fraction and controlling growth of polymer chains by switching on/off the UV light.

Another approach for photoinitiated ATRP was realized by using heterogeneous nanoparticles as photoactivator. Semiconductor nanoparticles are known as light-sensitive compounds that can be excited upon irradiation and consequently releasing their electrons in the conductive bond. Zhou and co-workers [53] reported UV-induced surface-initiated ATRP using TiO_2 nanoparticles in the water/methanol medium. The polymerization process was initiated from the initiator-modified substrate thus forming polymer brushes. The thickness of the polymer brush was increased linearly as a function of irradiation time. It has been observed that various monomers such as 3-sulfopropyl methacrylate potassium salt (SPMA), 2-hydroxyethyl methacrylate, DMAEMA, N-isopropylacrylamide and oligo (ethylene glycol) methacrylate were successfully polymerized using TiO_2 nanoparticles in conjunction with $Cu^{II}Cl_2/(Bipy)_2$ as the catalyst system. Furthermore, the block copolymer brushes were then successfully synthesized by using PDMAEMA brushes as macroinitiators in further polymerization of SPMA monomer.

The same group also developed a similar system to achieve photopatterned brushes utilizing dye-sensitized TiO_2 nanoparticles, which upon irradiation in the visible light range led to the injection of the photoexcited electrons from dye into the conduction band of nanoparticles. Subsequently, the excited electrons from the nanoparticles formed activator Cu(I) species from the deactivator Cu(II) initiating the polymerization process [54]. Figure 2.10 shows a schematic illustration of polymer brush growth in a photoinduced ATRP process using dye-sensitized TiO2 NPs as photocatalyst.

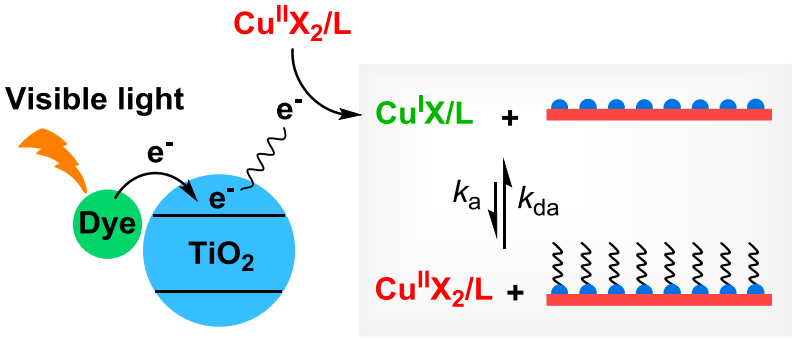

Figure 2.10 : Schematic illustration of the growth of polymer brush by photoinitiated ATRP using dye-sensitized TiO_2 nanoparticles.

3. EXPERIMENTAL PART

3.1 Materials

Methyl methacrylate (MMA, 99%; Sigma-Aldrich) was purified by passing through a basic alumina column to remove inhibitor.

N,N,N′,N″,N″-Pentamethyldiethylenetriamine (PMDETA, 99%; Sigma-Aldrich) was distilled prior to use.

Acryl amide (AAm, Fluka) was used as received. Poly(ethylene glycol) diacrylate (PEGDA, M_n = 575 g mol^{-1}) was purchased from Sigma-Aldrich and used as received. Triethylamine (TEA, Sigma-Aldrich) was used as received.

Diphenyliodonium hexafluorophosphate ($Ph_2I^+PF_6^-$, 98%; Alfa Aesar), was used as received.

Ethyl α-bromoisobutyrate (EBiB, 98%; Sigma-Aldrich) was used as received.

Copper (II) bromide ($Cu^{II}Br_2$, 99%; Acros) used as received.

Iron (III) nitrate nonahydrate ($Fe^{III}(NO_3)_3.9H_2O$, 98%; Sigma-Aldrich) used as received.

Zinc (II) nitrate hexahydrate ($Zn^{II}(NO_3)_2.6H_2O$, 98%; Sigma-Aldrich) were used as received without any further purification.

All other chemicals and solvents were of reagent grade, purchased from Merck and used as received.

3.2 Instrumentation

3.2.1 Light source

Rayonet merry-go-round photoreactor equipped with 16 lamps emitting nominally at λ > 350 nm with a light intensity of 22 mW cm^{-2}. The light intensity was measured by Delta ohm HD-9021 power meter.

3.2.2 UV-vis spectrometer

UV-visible spectra were recorded with a Shimadzu UV-1601 spectrometer.

3.2.3 ^{1}H Nuclear magnetic resonance spectroscopy

^{1}H NMR spectra of 5–10 % (w/w) solutions in $CDCl_3$ with $Si(CH_3)_4$ as an internal standard were recorded at room temperature at 500 MHz on a Bruker DPX 250 spectrometer.

3.2.4 Field emission scanning electron microscopy

The surface morphology of the nanoparticles was studied using a JEOL Scanning Electron Microscope (JSM-7600F, Japan). X-ray diffraction patterns (XRD) were taken with a computer controlled X'Pert Explorer, PANalytical diffractometer.

3.2.5 Gel permeation chromatography

Molecular weights of polymers were measured with a gel permeation chromatography (GPC) on a ViscotekGPCmaxautosampler system consisting of a pump, a Viscotek UV detector, and Viscotek a differential refractive index (RI) detector with three ViscoGEL GPC columns (G2000H HR, G3000H HR, and G4000H HR, 7.8 mm internal diameter, 300 mm length) in series. The effective molecular weight ranges were 456 − 42800, 1050 − 107000, and 10200 − 2890000, respectively. THF was used as an eluent at flow rate of 1.0 mL min−1 at 30 °C. Both detectors were calibrated with PS standards having narrow-molecular-weight distribution. Data were analyzed using ViscotekOmniSEC Omni-01 software.

Number-average molecular weights of the water-soluble polymers were estimated by measurements of solution viscosity in water at 25 °C using Mark-Houwink parameters for polyacrylamide[55] as follows (Eq. 1):

$$[\eta] = 6.31\times10^{-3} M_n^{\,0.8} \qquad \textbf{(3.1)}$$

3.2.6 Photodifferential scanning calorimetry

Photodifferential scanning calorimetry (photo-DSC) measurements were carried out by means of a modified Perkin-Elmer Diamond DSC equipped with a Polilight

PL400 Forensic Plus light source between 320 and 500 nm. A uniform UV light intensity is delivered across the DSC cell to the sample and reference pans. The intensity of the light was measured as 40 mW cm^{-2} by a UV radiometer covering broad UV range. The measurements were carried out in an isothermal mode at 25 °C with a nitrogen flow of 20 mL min^{-1}.

3.3 Preparation Methods

3.3.1 Synthesis of nanoparticles

3.3.1.1 Synthesis of zinc oxide nanoparticles

Zinc oxide nanoparticles (ZnO NPs) were synthesized by simple hydrothermal method using the aqueous (DI water) mixtures of zinc chloride and ammonium hydroxide as source materials. In a typical reaction process, ammonium hydroxide solution was added drop wise in 0.1 M zinc chloride solution made in 100 mL of DI water under constant stirring. The addition of ammonium hydroxide was stopped when the pH of the solution reached 10.2. The reaction mixture was then continuously stirred for 1 more hour and the resultant solution was then transferred into a Teflon-lined autoclave and heated up to 150 oC for 3 h. After terminating the reaction, the autoclave was allowed to cool at room temperature and finally white precipitates were obtained which were washed with methanol several times and dried at room temperature.

The dried products were then calcined at 400 °C for 3 h and characterized in detail in terms of their structural, optical, photocatalytic and sensing properties.

3.3.1.2 Synthesis of iron doped zinc oxide nanoparticles

The synthesis of iron doped zinc oxide nanoparticles was quite similar to that of neat zinc oxide nanoparticles. Iron (III) nitrate and zinc (II) nitrate (1:3) were totally liquefied at ambient temperature and adjusted the pH of the resulted solution above 10.0 by drop wise addition of 0.2 M NaOH solution with constant vigorous stirring. The resulted basic solution was stirred overnight at 60 ^{o}C and centrifuged the precipitate at 2000 rpm. Discarded the supernatant solution and saved the precipitate. Washed precipitate with ethanol for three times and then allowed them to dry first at

ambient temperature and then in oven at 60 ^{o}C. Grinded the precipitate and stored in a clean, dry and inert plastic vials.

3.3.2 Photopolymerizations

3.3.2.1 Free radical polymerization in aqueous media

AAm (150 mg, 2.11 mmol), distilled water (0.5 mL) and ZnO NPs (5 mg) were added into a glass vial. The mixture was degassed with high purity nitrogen for 30 s and tightly closed. The content was irradiated in Rayonet merry-go-round photoreactor equipped with 16 lamps emitting nominally at $\lambda > 350$ nm with a light intensity of 22 mW cm^{-2}. The light intensity was measured by Delta ohm HD-9021 power meter. After irradiation, the bulk solid was dissolved in water (15 mL), and the NPs were separated by centrifugation. Finally, the polymer solution was precipitated in acetone and polymers were dried in vacuum for 24 h.

3.3.2.2 Model reaction

In order to prove the proposed initiation mechanism in aqueous environment, a model reaction was conducted using a non-polymerizable monomer. In a typical experiment, 1,1-diphenylethylene (0.5 mL) was dissolved in acetonitrile (1 mL) and distilled water (0.5 mL) was added drop wise until appearance of transparent one and phase solution. The mixture was degassed with high purity nitrogen for 30 s and irradiated under UV light for 24 h. After the separation of ZnO NPs by centrifugation, the formed compound was extracted from aqueous phase as follows. First, some water was added to the mixture to make organic-aqueous phase separation. Then, 2 mL chloroform was added to extract the photolysis product from aqueous phase to organic phase. This was repeated with other organic solvents such as diethylether, toluene, and ethylacetate to make sure the complete extraction of the product from the aqueous phase. Finally, separated organic solutions were merged and excess solvents were evaporated.

3.3.2.3 Free radical polymerization in organic media

In a typical polymerization run, ZnO NPs (5 mg) were added to the mixture of MMA (0.5 mL, 9.35 M) and TEA (20 µL, 0.143 mmol) or Ph_2I^+ PF_6^- (10 mg, 0.023 mmol) and then the polymerization mixture was degassed with ultra-high pure nitrogen gas

for 10 min and closed tightly to prevent air. The mixture was irradiated under UV-light. Afetr irradiation, polymers were precipitated into methanol and dried in vacuum

3.3.2.4 Kinetics studies by photo-DSC in aqueous media

To a solution of PEGDA (0.5 ml) in a few drops of water was added ZnO NPs (15 µL, 0.1 mmol) and NPs (0.05 mmol). Approximately 10 mg of this solution was transferred to a photo-DSC pan. Before irradiation, it was stabilized by keeping the sample in the dark for 1 min, after which irradiation was started in an isothermal mode at 25 °C without N_2 flow. The obtained heat is relative to the number of reacted double bonds and the rate of polymerization can be calculated according to:

$$R_p = \left(Q_t\right) \times 1000 / \left(n \times E_{db}\right) \quad \textbf{(3.2)}$$

where Q_t (J mol^{-1} s^{-1}) is the amount of released heat at time t, n the number of acrylate double bond, and E_{db} (kJ mol^{-1}) is the energy of double bond (~86 kJ mol^{-1}). By integrating **(3.2)**, double bond conversion was calculated. Calculations were made after baseline corrections.

3.3.2.5 Kinetics studies by photo-DSC in organic media

In 0.5 mL of PEGDA ZnO NPs (15 µL, 0.1 mmol) were added and approximately 10 mg of this solution was transferred to a photo-DSC pan. The sample was kept under nitrogen flow for at least 5 min to exclude oxygen from the solution.Before irradiation, it was stabilized by keeping the sample in the dark for 1 min, after which irradiation was started in an isothermal mode at 25 °C. The conversions were calculated according to **(3.2)**.

3.3.2.6 Atom transfer radical polymerization

MMA (2 mL, 18.6 mmol), PMDETA (58.2 µL, 0.279 mmol), $Cu^{II}Br_2$ (20.7 mg, 0.093 mmol), EBiB (13 µL, 0.093 mmol), acetonitrile (0.5 mL, 9.57 mmol), and ZnO NPs (7.6 mg, 0.093 mmol) were placed into a Schlenk tube, and the reaction mixture was degassed by two freeze-pump-thaw cycles and left in vacuum. The mixture was irradiated under UV light. The resulted polymers were precipitated in methanol and then dried under vacuum.

Chain extension was performed employing with $[MMA]_0/[PMMA\text{-}Br]_0/[Cu^{II}Br_2]_0/[PMDETA]_0/[ZnO]_0$ = 400/1/1/3/1. A macroinitiator prepared by photoinduced ATRP after 1h, PMMA-Br ($M_{n,GPC}$ = 2000, M_w/M_n = 1.15; 0.18 g, 9.3×10^{-2} mmol), MMA (4 mL, 37.2 mmol), PMDETA (5.8 µL, 2.8×10^{-3} mmol), and $Cu^{II}Br_2$ (20 mg, 9.3×10^{-2} mmol) were put into a Schlenk tube, and the reaction mixture was degassed by three freeze–pump–thaw cycles and left in vacuum. The mixture was irradiated under the same experimental condition and the reaction was ceased after 7 h by opening the flask and precipitated in the methanol. Finally, the obtained polymer was dried under reduced pressure (conversion: 48%, $M_{n,GPC}$ = 22000, M_w/M_n = 1.22).

4. RESULTS AND DISCUSSION

There has been an interest in (photo)polymer community in developing long wavelength [56, 57] photoinitiating systems working under mild conditions (e.g. the use of LED light sources [58] or oxygen tolerable systems [59, 60]) with low energy consumptions [9, 61]. As an example, semiconducting porous organic and inorganic nanoparticles (NPs) are being introduced as efficient photoinitiators in various photopolymerization fields [44, 62-64]. Semiconductor NPs, for example zinc oxide and titanium dioxide NPs, have already been in extreme use of environmetal applications. The mechanism of dye degradation in aqueous media with the aid of NPs involving formation of active radical sites through interaction of the photogenerated electrons and holes with oxygen and water molecules, inspired use to xamine the photocatalytic applicability of these materlas in polymerization systems.

We chose to go with ZnO and iron doped zinc oxide (Fe/ZnO) NPs synthesized through a simple hydrothermal process of the aqueous solutions of zinc chloride and ammonium hydroxide [65]. The study includes two systems of photoinitiated conventional and controlled radical polymerizations: free radical and atom transfer radical polymerizations (ATRP).

4.1 Photoinitiated Free Radical Polymerization Using ZnO NPs

The obtained ZnO and Fe/ZnO NPs were in form of monodisperse spherical paricles with the average particle size of 50 and 20 nm, respectively. FESEM images of ZnO and Fe/ZnO NPs are shown in Figure 4.1. In the crystallinity evaluations both ZnO and Fe/ZnO nanoparticles exhibited identical peaks as that of Wurtzite hexagonal ZnO NPs, whereas Fe/ZnO NPs have a small shift toward low two theta which might be due to change in lattice spacing of ZnO caused by Fe doping (Figure 4.2) [66-69].

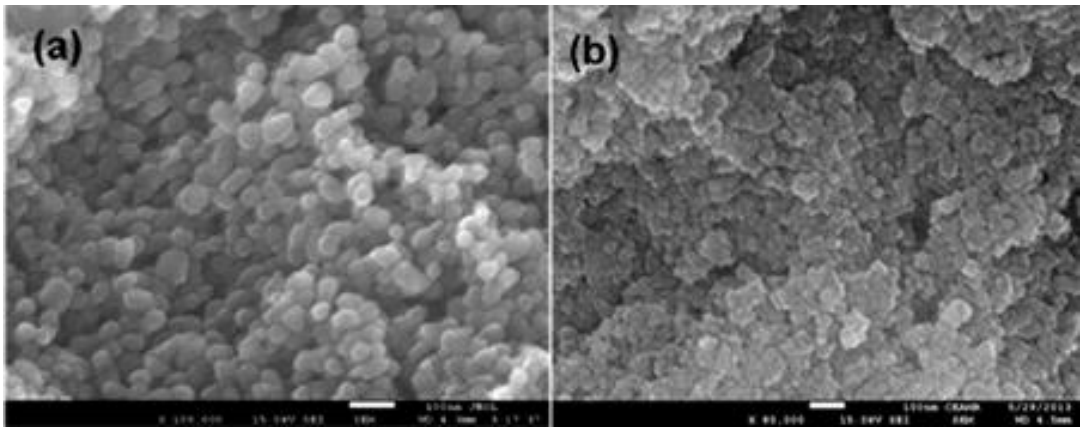

Figure 4.1 : FESEM images of (a) ZnO and (b) Fe/ZnO NPs.

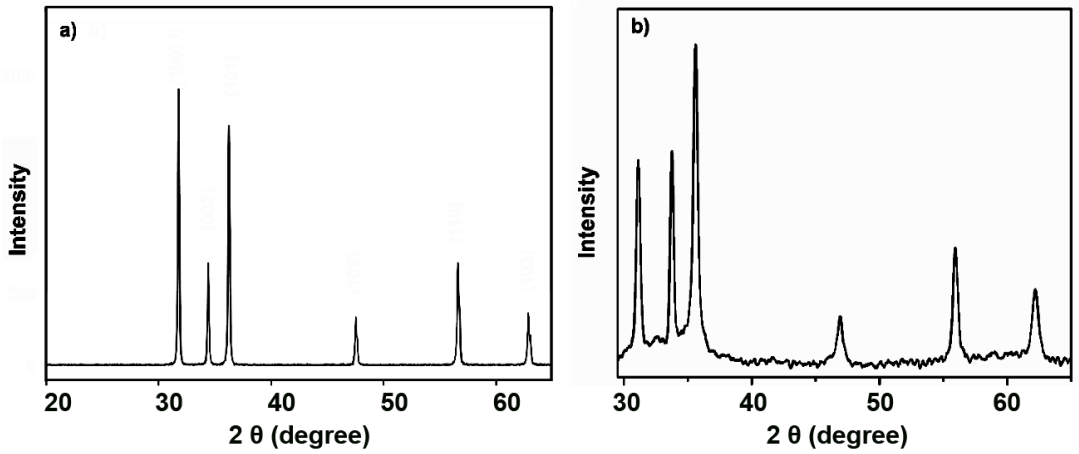

Figure 4.2 : Typical XRD spectra of (a) ZnO and (b) Fe/ZnO NPs.

To take the advantage of the synthesized NPs in photopolymerization, first, their optical properties in the UV-visible range were studied by UV-vis spectroscopy. As shown in Figure 4.3, ZnO NPs have an absorbance peak around 375 nm in the UV region, which is in well agreement with the theoretical calculation (~375 nm). In addition, Fe doped ZnO (Fe/ZnO) shows higher absorbance in this area with compared to ZnO NPs as well as a very broad, but weak, peak in the visible region. This higher absorbance of Fe/ZnO NPs promotes higher photolysis activity of these particles, with respect to ZnO.

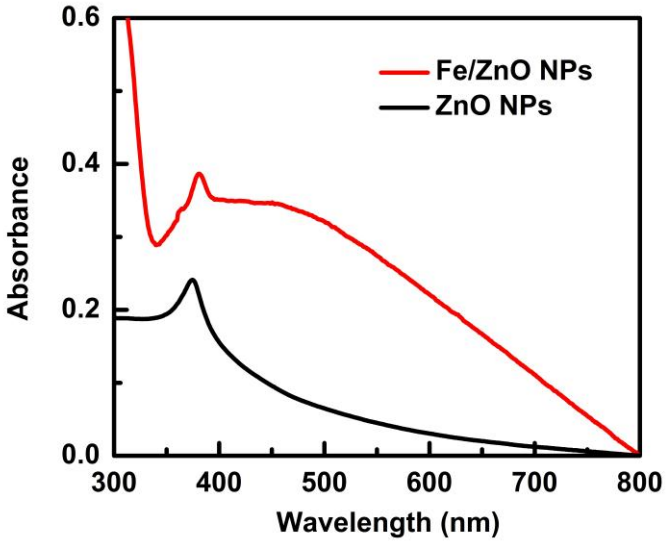

Figure 4.3 : UV-vis spectra of ZnO and Fe/ZnO NPs measured in acetonitrile.

4.1.1 Photopolymerization in aqueous media

In a typical polymerization run in an open tube (10 mL) without any degassing, due to the high concentration of O_2 in the system, no polymerization took place. Therefore, the system was degassed with high pure nitrogen gas for 30 s to decrease the concentration of oxygen present in the system. Acrylamide (AAm) monomer was chosen as a water-soluble monomer. Typical results of the photopolymerization of AAm in aqueous environment are collected in Table 4.1. Both ZnO and Fe/ZnO NPs were effective in the initiating of polymerization though Fe/ZnO NPs showed higher activity. Apparently, no polymer is formed in the absence of NPa, as well as in the presence of high concentration of O_2 that quenches the initiating radicals (Table 4.1, Runs 1 and 2). Remarkably, when the solvent was changed to THF the system failed to produce any polymer, indicating the role of water in the formation of initiating radicals (Run 5, Table 4.1).

In order to have a better understanding of the kinetics of photopolymerizations induced by these NPs, photocuring of poly(ethylene glycol) diacrylate (PEGDA) with NPs in aqueous media was studied using photo-DSC. Figure 4.4 shows the polymerization rate and real-time double bond conversion.

Photo-DSC results presented in Figure 4.4 show higher the efficiency of Fe/ZnO NPs in terms of higher polymerization rate and double bond conversion compared with ZnO NPs.

Table 4.1 : UV-light induced polymerization of AAm using ZnO or Fe/ZnO NPs in aqueous environment at room temperature.

Run[a]	Type of NPs	Degassing Time (s)	Gelation Time (min)	Conversion (%) [b]	M_n (g mol^{-1})[c]
1	-	30	-	-	-
2	ZnO or Fe/ZnO	-	-	-	-
3	ZnO	30	<7	55	56,000
4	Fe/ZnO	30	<5	60	60,000
5[d]	ZnO or Fe/ZnO	-	-	-	-

[a]λ > 350 nm, [AAm] = 4.22 M. [b]Measured gravimetrically. [c]Number average molecular weight (M_n) determined by viscosimetry method (Eq.1). [d]The experiment was performed in THF instead of water under N_2 atmosphere.

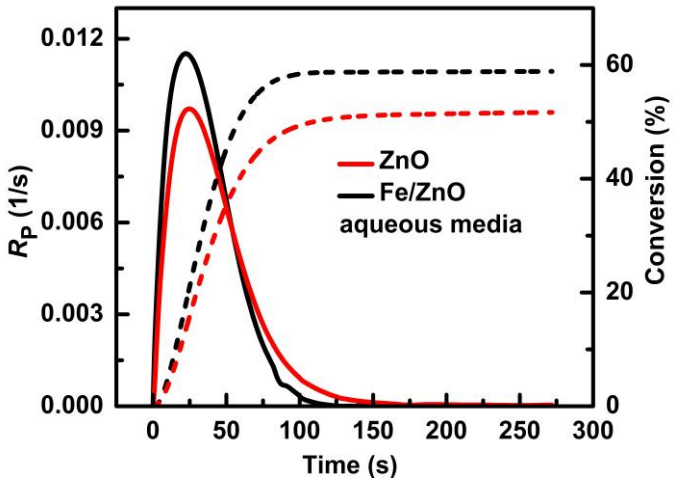

Figure 4.4 : Kinetic of the photopolymerization of PEGDA using semiconductor NPs in aqueous environment obtained by photo-DSC. Solid lines: rate of polymerization, R_P (1/s); dashed lines: conversion (%).

An initiation mechanism based on the formation of hydroxyl radicals as a result of the interaction of the photogenerated charge carriers from semiconductor with water and oxygen in the media. To prove this, a model reaction was conducted using a non-polymerizable monomer, 1,1-diphenylethylene, under the same experimental conditions. Diphenyl methyl radicals formed by the addition of initiating radicals have low reactivity [70] and are expected to couple [71] (Figure 4.5). The ^{1}H NMR spectra of the resulted product from the model reaction (Figure 4.6) represent a resonance of proton of hydroxyl groups around 4.8 confirming the crucial role of the hydroxyl radicals in the initiation process. Expectedly, proton exchange results in the disappearance of this peak.

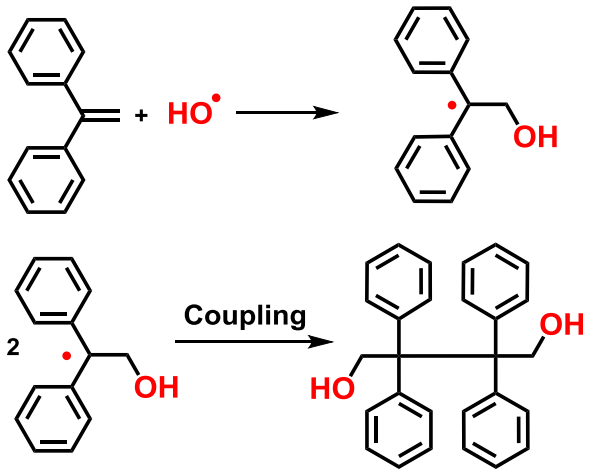

Figure 4.5 : Combination of the diphenyl methyl radicals formed in the model reaction.

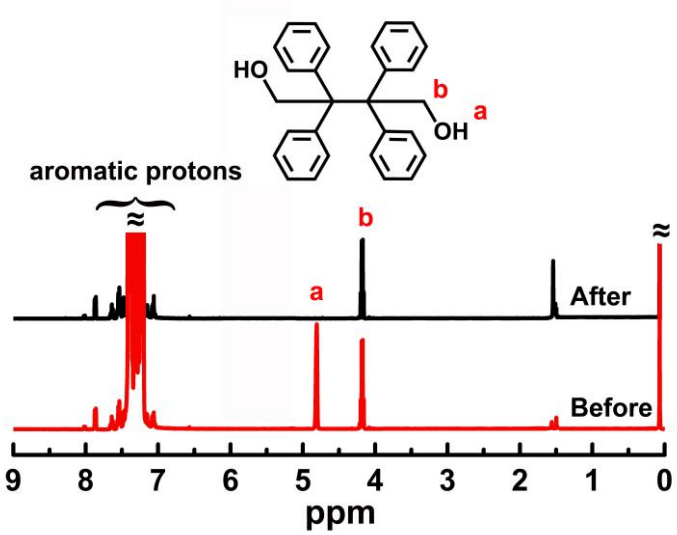

Figure 4.6 : ^{1}H NMR spectra of the coupled product of the model reaction before (bottom) and after (top) proton exchange.

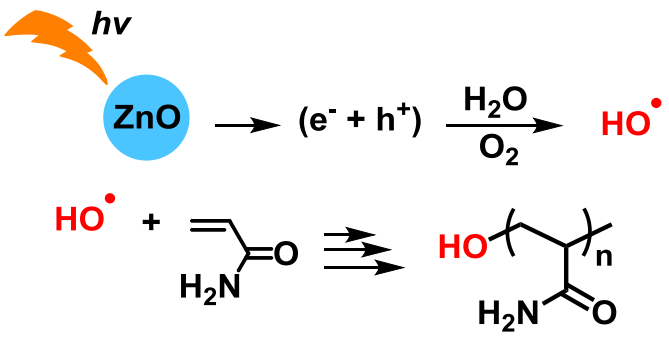

Figure 4.7 : Photopolymerization of AAm using semiconductor NPs in aqueous environment.

Based on these results, the mechanism of photopolymerization of AAm using ZnO NPs in aqueous media can be related to the formation of hydroxyl radicals stemmed through interaction of the photogenerated holes and electrons from ZnO with water and oxygen molecules present in the media. The photogenerated holes tend to oxidize water to form hydroxyl radicals, while in the second pathway the electrons can also react with oxygen molecules and after a set of reactions, hydroxyl radicals are schived , as shown in Figure 4.7.

An additional advantage of the initiating system described is related to the simple separation of the main components, ZnO or Fe/ZnO NPs from the mixture after the polymerization, which can be purified and reused as photoinitiator in further polymerizations. As can be seen from Figure 4.8, after several uses in the photopolymerization, the NPs retain their activity.

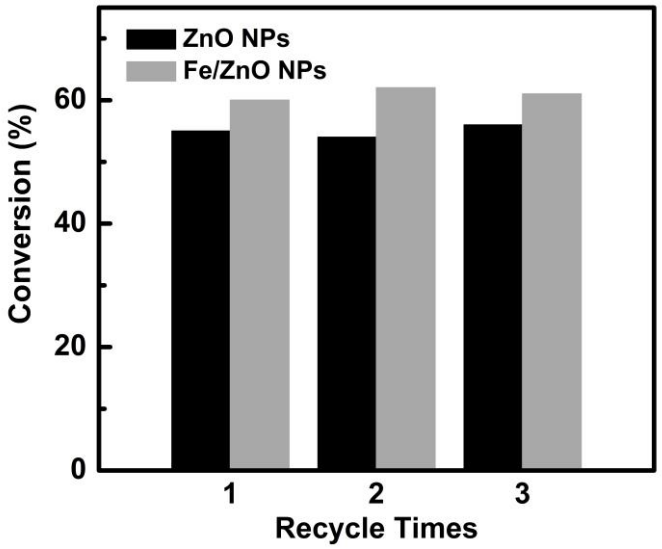

Figure 4.8 : Repeated use of ZnO or Fe/ZnO NPs in photopolymerization of AAm in aqueous media.

4.1.2 Photopolymerization in organic media

We have also examined photopolymerization of methyl methacrylate (MMA) as an oil-soluble monomer employing two different co-initiators. Control experiments in the absence of either NPs or co-initiator resulted in no polymerization indicative of the necessity of those components and light for a successful initiation (Table 4.2). This indicates that the released electrons or holes received by the co-initiators and not by the monomer itself, resulting in the formation of reactive radicals capable of initiating the polymerization. In the case of TEA as co-initiator, the polymerization

proceeds in a similar mechanism that described for mpg-C_3N_4 [10]. The oxidation of amine by photochemically formed holes to the corresponding radical cation, which abstracts hydrogen from another amine to form initiating radicals.

In the case of the iodonium salt, however, a different situation is encountered. The direct reduction of the iodonium salt by the released electron is responsible for the initiation. The overall mechanism is presented in Figure 4.9.

Table 4.2 : UV-light induced polymerization of MMA using ZnO or Fe/ZnO NPs in organic environment at room temperature.

Run[a]	Type of NPs	Co-initiator	Conversion (%)[b]	$M_n \times 10^{-3}$ (g mol^{-1})[c]	M_w/M_n[c]
1	-	TEA	-	-	-
2	-	Ph_2I^+ PF_6^-	-	-	-
3	ZnO or Fe/ZnO	-	-	-	-
4	ZnO	TEA	30	115.2	2.40
5	Fe/ZnO	TEA	36	210.0	2.85
6	ZnO	Ph_2I^+ PF_6^-	31	113.2	3.10
7	Fe/ZnO	Ph_2I^+ PF_6^-	27	141.5	3.65

[a] λ_{irr} > 350 nm; Irradiation Time: 10 min for TEA, and 240 min for Ph_2I^+ PF_6^-, [MMA] = 9.35 M, [TEA] = 0.256 M, [Ph_2I^+ PF_6^-] = 0.023 M, b Measured gravimetrically, c Number average molecular weight (M_n) and molecular weight distribution (M_w/M_n) determined by GPC.

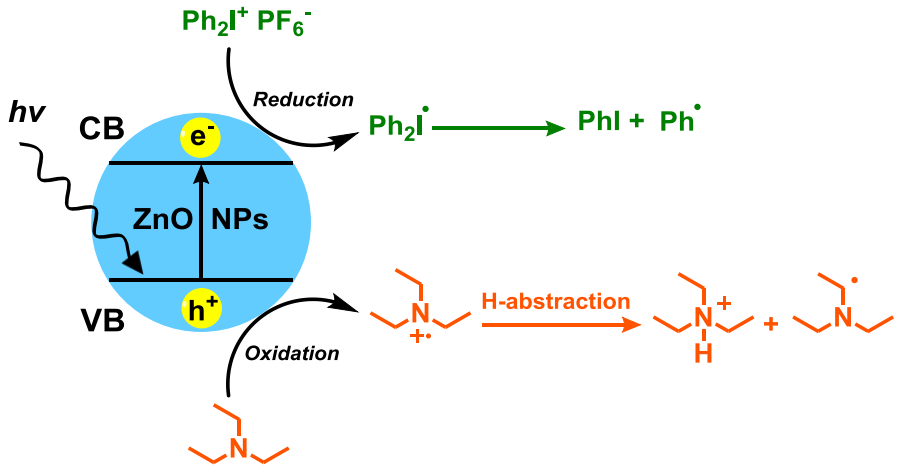

Figure 4.9 : Mechanism of formation of initiating free radicals in photopolymerization of MMA using ZnO NPs in the presence of iodonium or amine co-initiators.

The kinetic of the photopolymerization of PEGDA in the presence of iodonium salt as co-initiator by using ZnO or Fe/ZnO was further followed by photo-DSC. The measurements were carried out in an isothermal mode at 25 ^{o}C under a nitrogen flow of 20 mL min^{-1}. Figure 4.10 shows the results of the photo-DSC measurements for the photopolymerization of PEGDA in the presence of iodonium salt co-initiator. The rate of polymerization with ZnO NPs is higher than that of Fe/ZnO in the rapid first stage until it comes to a maximum. Afterwards, in the slow second stage, the rate of polymerization with Fe/ZnO NPs decreases more slowly than that of ZnO NPs, allowing it again to reach high conversions.

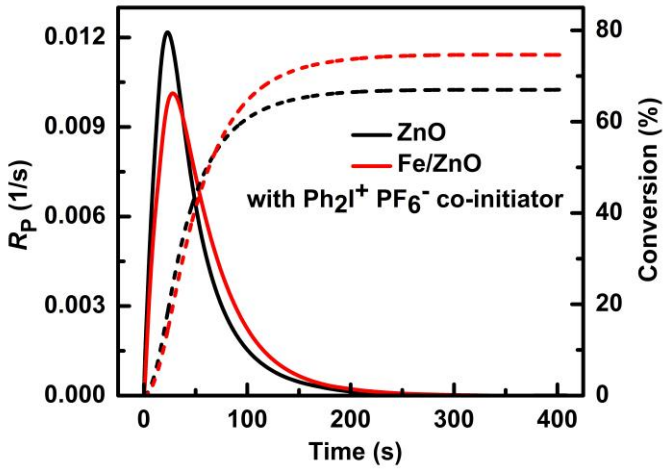

Figure 4.10 : Kinetics of photopolymerization of PEGDA using semiconductor nanoparticles in the presence of iodonium salt obtained by photo-DSC. Solid lines: rate of polymerization, R_P (1/s); dashed lines: conversion (%).

We have also tested the efficiency of the initiating system described in cationic polymerization. Iodonium salts are known as suitable photoinitiators for cationic polymerization of appropriate monomers. Irradiation of the mixture of cyclohexene oxide (CHO) monomer, $Ph_2I^+PF_6^-$ and ZnO or Fe/ZnO, failed to produce any polymer. This is expected since the reduction of the iodonium salt by the released electrons generates only radicals but not cationic species.

4.2 Photoinitiated ATRP using ZnO NPs

In order to take advantage of the use of ZnO nanoparticles in the polymerization, first, optical properties of reaction mixture (MMA/$Cu^{II}Br_2$/PMDETA), ZnO and iron

doped zinc oxide (Fe/ZnO) nanoparticles in the UV-visible range have been examined by UV-vis spectroscopy. As shown in Figure 4.11, at the irradiation wave-

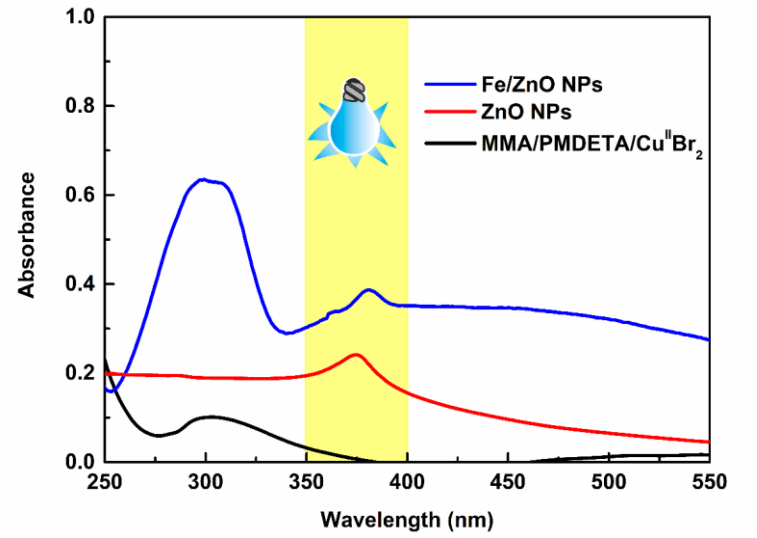

Figure 4.11 : UV–vis spectra of ZnO and Fe/ZnO nanoparticles, and reaction mixture in acetonitrile. The concentration of both ZnO and Fe/ZnO nanoparticles was 3×10^{-6} M and the system was 3×10^{-4} M.

length only ZnO and Fe/ZnO nanoparticles absorb the light where the other components of the reaction mixture are completely transparent.

Initially, the polymerization of methyl methacrylate (MMA) was examined by using the $Cu^{II}Br_2$/PMDETA as the catalyst, ethyl α-bromoisobutyrate (EBiB) as the initiator and ZnO nanoparticles as the photosensitive compound. During UV irradiation, ZnO nanoparticles easily absorb photons and promote electrons from the valence bands to the conduction bands, and then the excited electrons can spontaneously reduce $Cu^{II}Br_2$−ligand to $Cu^{I}Br$−ligand, which operates the ATRP of MMA. In order to confirm the initiating mechanism, various control experiments including those in the absence of nanoparticle, Cu^{II} or alkyl halide were conducted to reveal the role of each component in the polymerization (Table 4.3). When the polymerizations were conducted in the absence of either ZnO nanoparticles or alkyl halide or $Cu^{II}Br_2$, the experiments failed to produce any polymer at the end of irradiation and each component is required for successful controlled radical polymerization. Polymerizations proceed only when the redox components were present in the system. Compared to neat ZnO nanoparticles, Fe/ZnO nanoparticles provided relatively fast polymerization rate with narrow molecular weight distribution (Table 4.3, entry 5). The addition of Fe in ZnO increased the absorbance

at higher wavelengths as well as enhanced rate of polymerization of the system. Previously, Fe doped ZnO nanoparticles showed higher photocatalytic efficiency for dye degradation than bare ZnO nanoparticles at the same time of illumination [72] .

Table 4.3 : The results of photoinduced ATRP of MMA using ZnO and Fe/ZnO NPs as photocatalyst.

Run[a]	$[M]_0/[RX]_0/[Cu^{II}]_0/[L]_0/[ZnO]$	NPs Type	Conv.[b] [%]	$M_{n,th}$[c] [g mol^{-1}]	$M_{n,GPC}$[d] [g mol^{-1}]	M_w/M_n[d]
1	200/1/1/3/0	-	-	-	-	-
2	200/0/1/3/1	ZnO	-	-	-	-
3	200/1/0/3/1	ZnO	-	-	-	-
4	200/1/1/3/1	ZnO	40	8,000	8,100	1.23
5	200/1/1/3/1	Fe/ZnO	57	11,400	11,900	1.18

[a]The samples were irradiated under UV light (350 nm), time = 3 h.; [b]Measured gravimetrically.; [c]$M_{n,th} = [M]_0/[RX]_0 \times M_{w,mon} \times$ conv.; [d]Number average molecular weight ($M_{n,GPC}$) and molecular weight distribution (M_w/M_n) were determined by gel permeation chromatography.

Based on the above results, the kinetic plot and the evolution of molecular weight and distribution with conversion for the photoinduced ATRP of MMA in the presence of ZnO (Figure 4.12) or Fe/ZnO (Figure 4.13) nanoparticles were investigated. In both cases, the linear relationship between monomer consumption, $\ln([M]_0/[M])$ with polymerization time indicated that the propagating radical concentrations were almost constant during the polymerization. Evolution of the molar mass (M_n) and molecular weight distribution (M_w/M_n) (Figure 4.12.b and Figure 4.13.b) show that during photoinduced ATRP of MMA with $[MMA]_0/[RX]_0/[MtX]_0/[L]_0/[ZnO]_0$ = 200/1/1/3/1 ratio, the polydispersity indexes in both cases were slightly broader (1.18−1.30). Moreover, the obtained molar masses were in good agreement with the theoretical values, indicating high initiation efficiency. Notably, Fe/ZnO nanoparticles allow a much faster ATRP and narrow polydispersity indexes over the polymer properties than ZnO nanoparticles.

Gel permeation chromatography (GPC) traces of the obtained polymers by ZnO and Fe/ZnO nanoparticles at different time intervals are presented in Figure 4.14. It can be seen that the molecular weight of the polymers asymmetrically shifted toward the

higher molecular weight region as the polymerization proceeded, indicating the existence of controlled growing species in both cases.

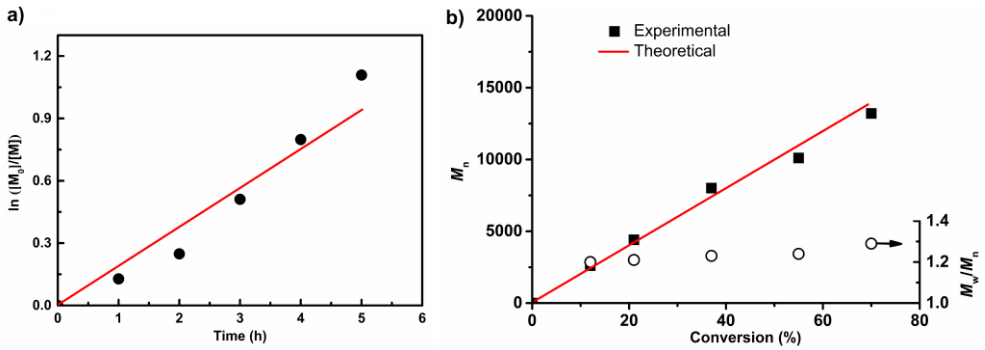

Figure 4.12 : Photoinduced ATRP of MMA with $[MMA]_0/[RX]_0/[MtX]_0/[L]_0/[ZnO]_0$ = 200/1/1/3/1 ratio a) kinetic plot and b) molecular weights and distributions of the resulting polymers as a function of degree of conversion.

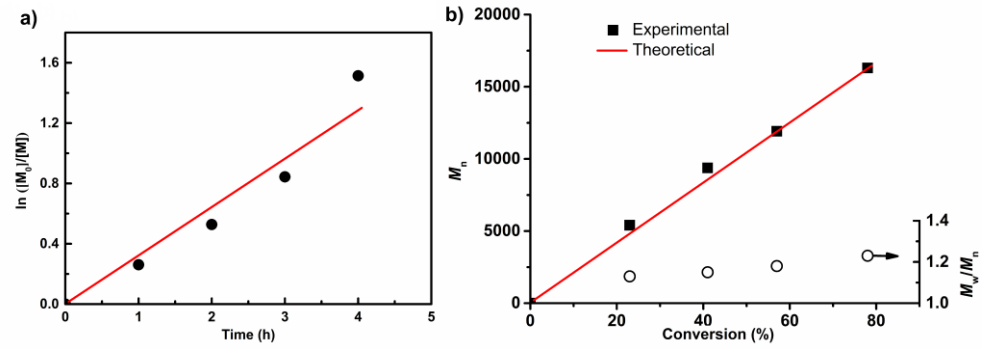

Figure 4.13 : Photoinduced ATRP of MMA with $[MMA]_0/[RX]_0/[MtX]_0/[L]_0/[Fe/ZnO]_0$ = 200/1/1/3/1 ratio a) kinetic plot and b) molecular weights and distributions of the resulting polymers as a function of degree of conversion.

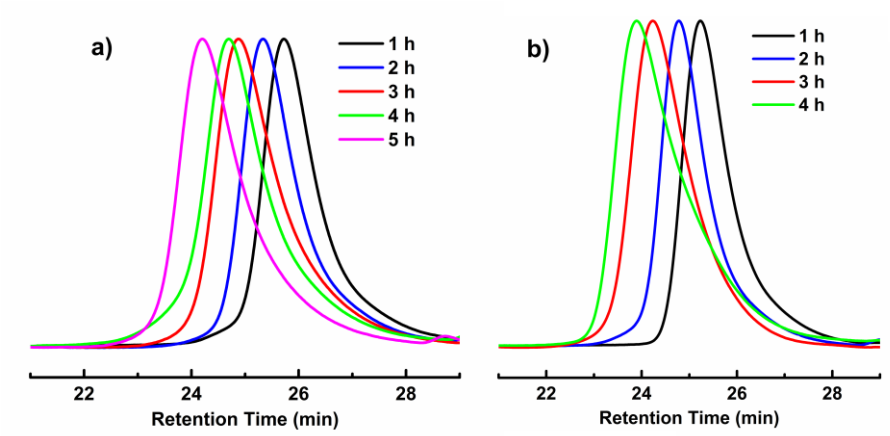

Figure 4.14 : Gel permeation chromatography (GPC) traces of the PMMAs using a) ZnO and b) Fe/ZnO nanoparticles as photocatalyst at different time intervals.

To further investigate the effect of UV light irradiation on the photoinduced polymerization of MMA, the light was turned on and off intermittently during the reaction (light off at 0-1, 2-3, and 4-5 h in Figure 4.15). Firstly, monomer, initiator, and catalyst were initially combined in the absence of light and after one hour, no polymerization was observed. The reaction was then exposed to UV light for one hour at room temperature, which resulted in approximately 13% monomer conversion. Thereafter, the light source was periodically turned-off and the polymerization proceeded at a much lower rate during this period, indicating a negligible concentration of the active radical present under dark conditions. Exposure to UV light for a second one-hour period "turns" the polymerization back on and this "on"/"off" cycle can be repeated numerous times with negligible reaction in the absence of irradiation. The gradual increase of the yield with the irradiation time clearly indicates that the polymerization is driven by light. The polymer yield increased only under the UV light irradiation while the polymerization stopped in the light-off period.

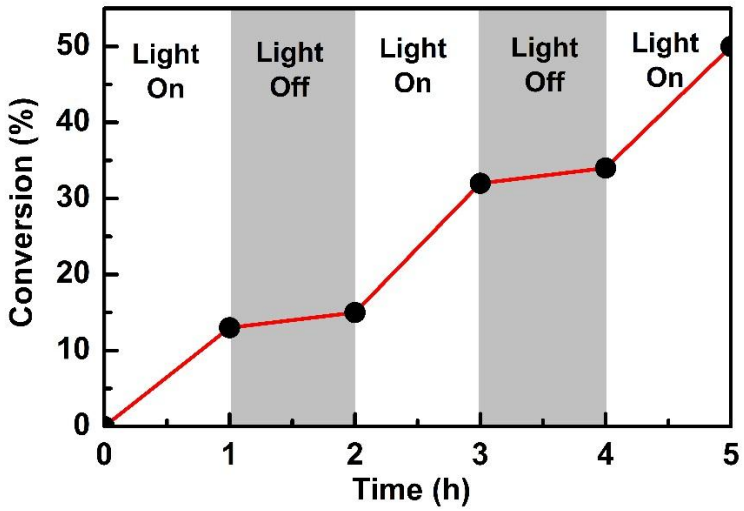

Figure 4.15 : Effect of UV light during the polymerization of MMA at room temperature; $[MMA]_0/[RX]_0/[MtX]_0/[L]_0/[ZnO]_0 = 200/1/1/3/1$.

The living nature of the system was further examined by treating the macroinitiator made by this technique with a same monomer for chain extension using the same conditions. For this purpose, a macroinitiator ($M_{n,GPC}$ = 2000 g mol^{-1}, PDI = 1.15) prepared by photoinduced ATRP was employed with $[MMA]_0/[PMMA\text{-}Br]_0/[Cu^{II}Br_2]_0/[PMDETA]_0/[ZnO]_0 = 400/1/1/3/1$ ratio in chain extension reaction. Figure 5 shows the GPC analysis of the samples taken during the chain extension

process before and after sequential monomer addition. As shown in Figure 4.16, the polymer chains were clearly shifted to higher molecular weights ($M_{n,GPC}$ = 22,000 g mol^{-1}, PDI = 1.22) and no detectable amount of unreacted initial block. Figure 4.17 shows a typical ^{1}H NMR spectra of the obtained PMMA homopolymer. A strong peak at 3.62 ppm (**a**) was assignable to the methoxy protons of PMMA. The small peak at 4.0 ppm (g) was assignable to the methylene protons of the initiator. The results of ^{1}H NMR analysis and chain extension demonstrated that well-defined PMMA bearing a halide group was synthesized via photoinduced ATRP.

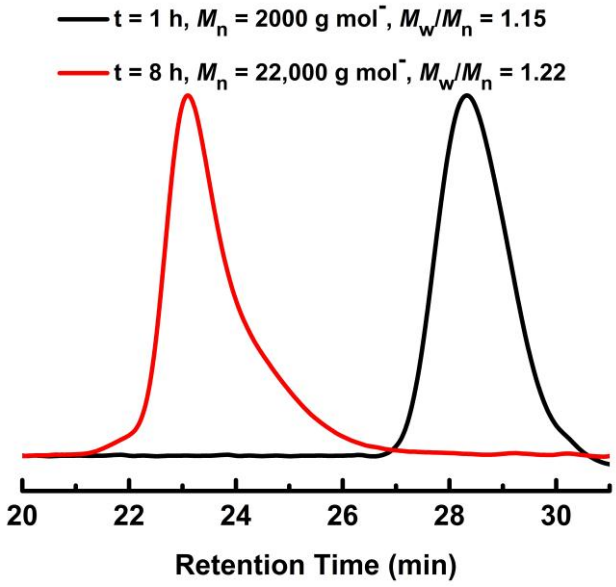

Figure 4.16 : GPC analysis of the samples during the chain extension process before (black line) and after (red line) sequential monomer addition.

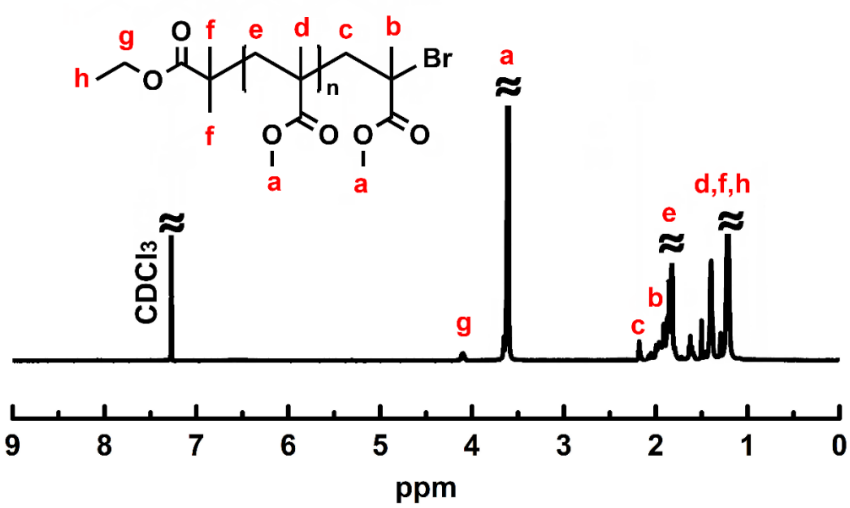

Figure 4.17 : ^{1}H NMR spectrum of PMMA synthesized by using ZnO nanoparticles as photocatalyst in photoinduced ATRP.

A possible mechanism for the polymerization should consider continuous regeneration of copper catalyst in an activator generated by electron transfer (AGET) ATRP mechanism as illustrated in Figure 4.18. The primary photochemical reaction involves the generation of a positive hole (h^+) and an electron (e^-), which are generated in conduction and valence bands, correspondingly. The valence band electrons reduced the Cu^{II}/L to Cu^{I}/L directly [73], which was used as activator in the AGET ATRP. Subsequently, polymerization was started by the activation of an R-X initiator by the Cu^{I}/L activator. Notably, each component of the system including ZnO nanoparticles or alkyl halide or $Cu^{II}Br_2$ or light irradiation is required for successful controlled radical polymerization.

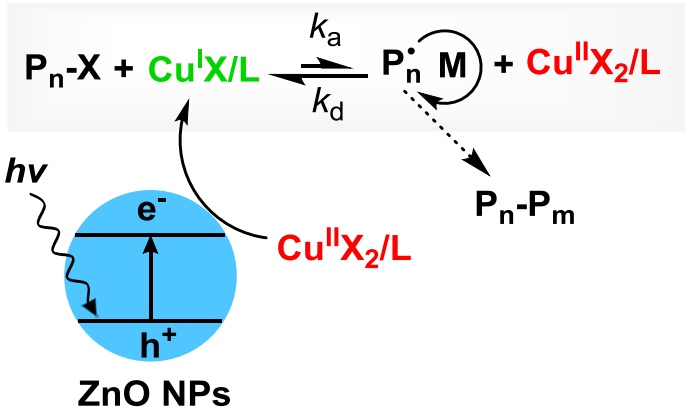

Figure 4.18 : Plausible photoinitiated ATRP using zinc oxide nanoparticles.

5. CONCLUSIONS

In summary, the photocatalytic applicability of semiconductor nanoparticles has been investigated in photopolymerization systems. ZnO and Fe/ZnO NPs have been used as heterogeneous photocatalyst in photoinitiated free radical and atom transfer radical polymerization techniques. The ability of these NPs to release electron-hole pairs upon photoexcitation was exploited to generate initiating free radicals in the free radical method in different media.

In aqueous media, photoredox processes of water and oxygen present in the system gave rise to active radicals, indicative of a potential method to overcome oxygen inhibition in photopolymerizations. For polymerizations in organic media (i.e. in the absence of water and oxygen), co-initiators were needed to accomplish the process. An amine and an iodonium salt co-initiator, independently, were reported to undergo reduction and oxidation reactions, respectively with the photogenerated holes and electrons from the semiconductor.

For the ATRP process, NPs were used to generate *in situ* the required Cu(I) catalyst for ATRP. The photogenerated electrons successfully reduced initially loaded air-stable Cu(II) species to Cu(I) to catalyze the reaction. Polymers with a good agreement of their molecular weights with theoretical values having narrow molecular weight distributions of 1.15-1.20 were obtained photochemically. Of course, the key advantage of such photoinitiated ATRP systems is the ability of gaining spatiotemporal control over the chain growth; that is it can be manipulated simply by taking out the light and have chain growth stopped or get it started by shining light on (temporal control) or making patterned, 3D surfaces (spatial control).

The area of semiconducting materials in different aspects of photopolymer community is not fully investigated and taken advantage of and there remains much more to explore.

REFERENCES

[1] Adams, D. M., Brus, L., Chidsey, C. E. D., Creager, S., Creutz, C., Kagan, C. R., Kamat, P. V., Lieberman, M., Lindsay, S., Marcus, R. A., Metzger, R. M., Michel-Beyerle, M. E., Miller, J. R., Newton, M. D., Rolison, D. R., Sankey, O., Schanze, K. S., Yardley, J. and Zhu, X. Y., 2003. Charge Transfer on the Nanoscale: Current Status. *Journal of Physical Chemistry B,* **107,** 6668-6697.

[2] Wen, F. and Li, C., 2013. Hybrid Artificial Photosynthetic Systems Comprising Semiconductors as Light Harvesters and Biomimetic Complexes as Molecular Cocatalysts. *Accounts of Chemical Research,* **46,** 2355-2364.

[3] Gill, R., Zayats, M. and Willner, I., 2008. Semiconductor Quantum Dots for Bioanalysis. *Angewandte Chemie International Edition,* **47,** 7602-7625.

[4] Hagfeldt, A., Boschloo, G., Sun, L. C., Kloo, L. and Pettersson, H., 2010. Dye-Sensitized Solar Cells. *Chemical Reviews,* **110,** 6595-6663.

[5] Hoffmann, M. R., Martin, S. T., Choi, W. Y. and Bahnemann, D. W., 1995. Environmental Applications of Semiconductor Photocatalysis. *Chemical Reviews,* **95,** 69-96.

[6] Zhang, H., Chen, G. and Bahnemann, D. W., 2009. Photoelectrocatalytic Materials for Environmental Applications. *Journal of Materials Chemistry,* **19,** 5089-5121.

[7] Kisch, H., 2013. Semiconductor Photocatalysismechanistic and Synthetic Aspects. *Angewandte Chemie International Edition,* **52,** 812-847.

[8] Qu, Y. and Duan, X., 2013. Progress, Challenge and Perspective of Heterogeneous Photocatalysts. *Chemical Society Reviews,* **42,** 2568-2580.

[9] Yagci, Y., Jockusch, S. and Turro, N. J., 2010. Photoinitiated Polymerization: Advances, Challenges, and Opportunities. *Macromolecules,* **43,** 6245-6260.

[10] Kiskan, B., Zhang, J. S., Wang, X. C., Antonietti, M. and Yagci, Y., 2012. Mesoporous Graphitic Carbon Nitride as a Heterogeneous Visible Light Photoinitiator for Radical Polymerization. *Acs Macro Letters,* **1,** 546-549.

[11] Qin, S. H., Qin, D. Q. and Qiu, K. Y., 2001. A Novel Photo Atom Transfer Radical Polymerization of Methyl Methacrylate. *New Journal of Chemistry,* **25,** 893-895.

[12] Ishizu, K. and Katsuhara, H., 2006. Diethyldithiocarbamate-Mediated Living Radical Polymerization and Development for Architecture of Nanostructured Polymers. *Designed Monomers and Polymers,* **9,** 99-115.

[13] Kwak, Y. and Matyjaszewski, K., 2010. Photoirradiated Atom Transfer Radical Polymerization with an Alkyl Dithiocarbamate at Ambient Temperature. *Macromolecules,* **43,** 5180-5183.

[14] Jakubowski, W., Min, K. and Matyjaszewski, K., 2006. Activators Regenerated by Electron Transfer for Atom Transfer Radical Polymerization of Styrene. *Macromolecules,* **39,** 39-45.

[15] Dong, H. C., Tang, W. and Matyjaszewski, K., 2007. Well-Defined High-Molecular-Weight Polyacrylonitrile Via Activators Regenerated by Electron Transfer Atrp. *Macromolecules,* **40,** 2974-2977.

[16] Jakubowski, W., Kirci-Denizli, B., Gil, R. R. and Matyjaszewski, K., 2008. Polystyrene with Improved Chain-End Functionality and Higher Molecular Weight by Arget Atrp. *Macromolecular Chemistry and Physics,* **209,** 32-39.

[17] Zhu, G. H., Zhang, L. F., Zhang, Z. B., Zhu, J., Tu, Y. F., Cheng, Z. P. and Zhu, X. L., 2011. Iron-Mediated Icar Atrp of Methyl Methacrylate. *Macromolecules,* **44,** 3233-3239.

[18] Abreu, C. M. R., Mendonca, P. V., Serra, A. C., Popov, A. V., Matyjaszewski, K., Guliashvili, T. and Coelho, J. F. J., 2012. Inorganic Sulfites: Efficient Reducing Agents and Supplemental Activators for Atom Transfer Radical Polymerization. *Acs Macro Letters,* **1,** 1308-1311.

[19] Matyjaszewski, K., Jakubowski, W., Min, K., Tang, W., Huang, J., Braunecker, W. A. and Tsarevsky, N. V., 2006. Diminishing Catalyst Concentration in Atom Transfer Radical Polymerization with Reducing Agents. *Proceedings of the National Academy of Sciences of the United States of America,* **103,** 15309-15314.

[20] Magenau, A. J. D., Strandwitz, N. C., Gennaro, A. and Matyjaszewski, K., 2011. Electrochemically Mediated Atom Transfer Radical Polymerization. *Science,* **332,** 81-84.

[21] Matyjaszewski, K., Tsarevsky, N. V., Braunecker, W. A., Dong, H., Huang, J., Jakubowski, W., Kwak, Y., Nicolay, R., Tang, W. and Yoon, J. A., 2007. Role of Cu-0 in Controlled/"Living" Radical Polymerization. *Macromolecules,* **40,** 7795-7806.

[22] Tasdelen, M. A., Uygun, M. and Yagci, Y., 2010. Photoinduced Controlled Radical Polymerization in Methanol. *Macromolecular Chemistry and Physics,* **211,** 2271-2275.

[23] Tasdelen, M. A., Uygun, M. and Yagci, Y., 2011. Photoinduced Controlled Radical Polymerization. *Macromolecular Rapid Communications,* **32,** 58-62.

[24] Tasdelen, M. A., Uygun, M. and Yagci, Y., 2011. Studies on Photoinduced Atrp in the Presence of Photoinitiator. *Macromolecular Chemistry and Physics,* **212,** 2036-2042.

[25] Tasdelen, M. A., Ciftci, M., Uygun, M. and Yagci, Y., 2012. Possibilities for Photoinduced Controlled Radical Polymerizations. In *Progress in Controlled Radical Polymerization: Mechanisms and Techniques,* Matyjaszewski, K., Sumerlin, B. S. and Tsarevsky, N. V., Eds.

[26] Konkolewicz, D., Schroeder, K., Buback, J., Bernhard, S. and Matyjaszewski, K., 2012. Visible Light and Sunlight Photoinduced Atrp with Ppm of Cu Catalyst. *Acs Macro Letters,* **1,** 1219-1223.

[27] Tasdelen, M. A. and Yagci, Y., 2011. Photochemical Methods for the Preparation of Complex Linear and Cross-Linked Macromolecular Structures. *Australian Journal of Chemistry,* **64,** 982-991.

[28] Guan, Z. B. and Smart, B., 2000. A Remarkable Visible Light Effect on Atom-Transfer Radical Polymerization. *Macromolecules,* **33,** 6904-6906.

[29] Moffett, J. W. and Zika, R. G., 1987. Reaction-Kinetics of Hydrogen-Peroxide with Copper and Iron in Seawater. *Environmental Science and Technology,* **21,** 804-810.

[30] Natarajan, P. and Ferraudi, G., 1981. Photochemical Properties of Copper(Ii) Amino-Acid Complexes. *Inorganic Chemistry,* **20,** 3708-3712.

[31] Natarajan, P., Chandrasekaran, K. and Santappa, M., 1976. New Initiator for Polymerization - Photopolymerization of Vinyl Monomers Using Cu(Ii) - Amino-Acid Chelates. *Journal of Polymer Science Part C-Polymer Letters,* **14,** 455-458.

[32] Namasivayam, C. and Natarajan, P., 1983. Kinetics of Photo-Polymerization of Acrylamide Initiated by Copper (Ii)-Bis(Amino Acid) Chelates in Aqueous-Solution .2. *Journal of Polymer Science Part A: Polymer Chemistry,* **21,** 1385-1400.

[33] Giuffrida, S., Condorelli, G. G., Costanzo, L. L., Fragala, I. L., Ventimiglia, G. and Vecchio, G., 2004. Photochemical Mechanism of the Formation of Nanometer-Sized Copper by Uv Irradiation of Ethanol Bis(2,4-Pentandionato)Copper(Ii) Solutions. *Chemistry of Materials,* **16,** 1260-1266.

[34] Hayase, K. and Zepp, R. G., 1991. Photolysis of Copper(Ii)-Amino Acid Complexes in Water. *Environmental Science and Technology,* **25,** 1273-1279.

[35] Mert, H., Tunca, U. and Hizal, G., 2006. Thiophenol Derivatives as a Reducing Agent for in Situ Generation of Cu(I) Species Via Electron Transfer Reaction in Copper-Catalyzed Living/Controlled Radical Polymerization of Styrene. *Journal of Polymer Science Part A: Polymer Chemistry,* **44,** 5923-5932.

[36] David, P. G. and Dasilva, P. A. C., 1985. Photoredox Chemistry of Chloro and Bromo Complexes of Copper(Ii) in Methanolic Medium. *Bulletin of the Chemical Society of Japan,* **58,** 3566-3569.

[37] Mosnacek, J. and Ilcikova, M., 2012. Photochemically Mediated Atom Transfer Radical Polymerization of Methyl Methacrylate Using Ppm Amounts of Catalyst. *Macromolecules,* **45,** 5859-5865.

[38] Anastasaki, A., Nikolaou, V., Zhang, Q., Burns, J., Samanta, S. R., Waldron, C., Haddleton, A. J., McHale, R., Fox, D., Percec, V., Wilson, P. and Haddleton, D. M., 2014. Copper(Ii)/Tertiary Amine Synergy in Photoinduced Living Radical Polymerization: Accelerated Synthesis of Omega-Functional and Alpha,Omega-Heterofunctional Poly(Acrylates). *Journal of the American Chemical Society,* **136,** 1141-1149.

[39] Anastasaki, A., Nikolaou, V., Simula, A., Godfrey, J., Li, M., Nurumbetov, G., Wilson, P. and Haddleton, D. M., 2014. Expanding the Scope of the Photoinduced Living Radical Polymerization of Acrylates in the Presence of Cubr2 and Me6-Tren. *Macromolecules,* **47,** 3852-3859.

[40] Anastasaki, A., Nikolaou, V., Pappas, G. S., Zhang, Q., Wan, C., Wilson, P., Davis, T. P., Whittaker, M. R. and Haddleton, D. M., 2014. Photoinduced Sequence-Control Via One Pot Living Radical Polymerization of Acrylates. *Chemical Science,* **5,** 3536-3542.

[41] Fors, B. P. and Hawker, C. J., 2012. Control of a Living Radical Polymerization of Methacrylates by Light. *Angewandte Chemie International Edition,* **51,** 8850-8853.

[42] Poelma, J. E., Fors, B. P., Meyers, G. F., Kramer, J. W. and Hawker, C. J., 2013. Fabrication of Complex Three-Dimensional Polymer Brush Nanostructures through Light-Mediated Living Radical Polymerization. *Angewandte Chemie International Edition,* **52,** 6844-6848.

[43] Fors, B. P., Poelma, J. E., Menyo, M. S., Robb, M. J., Spokoyny, D. M., Kramer, J. W., Waite, J. H. and Hawker, C. J., 2013. Fabrication of Unique Chemical Patterns and Concentration Gradients with Visible Light. *Journal of the American Chemical Society,* **135,** 14106-14109.

[44] Dadashi-Silab, S., Tasdelen, M. A., Kiskan, B., Wang, X., Antonietti, M. and Yagci, Y., 2014. Photochemically Mediated Atom Transfer Radical Polymerization Using Polymeric Semiconductor Mesoporous Graphitic Carbon Nitride. *Macromolecular Chemistry and Physics,* **215,** 675-681.

[45] Taskin, O. S., Yilmaz, G., Tasdelen, M. A. and Yagci, Y., 2014. Photoinduced Reverse Atom Transfer Radical Polymerization of Methyl Methacrylate Using Camphorquinone/Benzhydrol System. *Polymer International,* **63,** 902-907.

[46] Tasdelen, M. A., Ciftci, M. and Yagci, Y., 2012. Visible Light-Induced Atom Transfer Radical Polymerization. *Macromolecular Chemistry and Physics,* **213,** 1391-1396.

[47] Ciftci, M., Tasdelen, M. A. and Yagci, Y., 2014. Sunlight Induced Atom Transfer Radical Polymerization by Using Dimanganese Decacarbonyl. *Polymer Chemistry,* **5,** 600-606.

[48] Iskin, B., Yilmaz, G. and Yagci, Y., 2013. Telechelic Polymers by Visible-Light-Induced Radical Coupling. *Macromolecular Chemistry and Physics,* **214,** 94-98.

[49] Ciftci, M., Batat, P., Demirel, A. L., Xu, G., Buchmeiser, M. and Yagci, Y., 2013. Visible Light-Induced Grafting from Polyolefins. *Macromolecules,* **46,** 6395-6401.

[50] Acik, G., Kahveci, M. U. and Yagci, Y., 2010. Synthesis of Block Copolymers by Combination of Atom Transfer Radical Polymerization and Visible Light Radical Photopolymerization Methods. *Macromolecules,* **43,** 9198-9201.

[51] Yagci, Y. and Hepuzer, Y., 1999. A Novel Visible Light Initiatiating System for Cationic Polymerization. *Macromolecules,* **32,** 6367-6370.

[52] Ciftci, M., Tasdelen, M. A., Li, W., Matyjaszewski, K. and Yagci, Y., 2013. Photoinitiated Atrp in Inverse Microemulsion. *Macromolecules,* **46,** 9537-9543.

[53] Yan, J. F., Li, B., Zhou, F. and Liu, W. M., 2013. Ultraviolet Light-Induced Surface-Initiated Atom-Transfer Radical Polymerization. *Acs Macro Letters,* **2,** 592-596.

[54] Li, B., Yu, B. and Zhou, F., 2014. Spatial Control over Brush Growth through Sunlight-Induced Atom Transfer Radical Polymerization Using Dye-Sensitized Tio2 as a Photocatalyst. *Macromolecular Rapid Communications,* **35,** 1287-1292.

[55] Brandrup, J. and Immergut, E. H., *Polymer Handbook.* J., B. and H., I. E., Eds. Wiley- Interscience Publication:

[56] Tunc, D. and Yagci, Y., 2011. Thioxanthone-Ethylcarbazole as a Soluble Visible Light Photoinitiator for Free Radical and Free Radical Promoted Cationic Polymerizations. *Polymer Chemistry,* **2,** 2557-2563.

[57] Tar, H., Esen, D. S., Aydin, M., Ley, C., Arsu, N. and Allonas, X., 2013. Panchromatic Type Ii Photoinitiator for Free Radical Polymerization Based on Thioxanthone Derivative. *Macromolecules,* **46,** 3266-3272.

[58] Zhang, J., Frigoli, M., Dumur, F., Xiao, P., Ronchi, L., Graff, B., Morlet-Savary, F., Fouassier, J. P., Gigmes, D. and Lalevee, J., 2014. Design of Novel Photoinitiators for Radical and Cationic Photopolymerizations under near Uv and Visible Leds (385, 395, and 405 Nm). *Macromolecules,* **47,** 2811-2819.

[59] Ligon, S. C., Husar, B., Wutzel, H., Holman, R. and Liska, R., 2014. Strategies to Reduce Oxygen Inhibition in Photoinduced Polymerization. *Chemical Reviews,* **114,** 557-589.

[60] Pynaert, R., Buguet, J., Croutxe-Barghorn, C., Moireau, P. and Allonas, X., 2013. Effect of Reactive Oxygen Species on the Kinetics of Free Radical Photopolymerization. *Polymer Chemistry,* **4,** 2475-2479.

[61] Fouassier, J.-P. and Lalevee, J., 2012. *Photoinitiators for Polymer Synthesis: Scope, Reactivity and Efficiency*. Wiley-VCH , Weinheim:

[62] Kiskan, B., Zhang, J., Wang, X., Antonietti, M. and Yagci, Y., 2012. Mesoporous Graphitic Carbon Nitride as a Heterogeneous Visible Light Photoinitiator for Radical Polymerization. *Acs Macro Letters,* **1,** 546-549.

[63] Yilmaz, G., Iskin, B., Yilmaz, F. and Yagci, Y., 2012. Visible Light-Induced Cationic Polymerization Using Fullerenes. *Acs Macro Letters,* **1,** 1212-1215.

[64] Wang, Z. J., Landfester, K. and Zhang, K. A. I., 2014. Hierarchically Porous Pi-Conjugated Polyhipe as a Heterogeneous Photoinitiator for Free Radical Polymerization under Visible Light. *Polymer Chemistry,* **5,** 3559-3562.

[65] Khan, S. B., Faisal, M., Rahman, M. M. and Jamal, A., 2011. Low-Temperature Growth of Zno Nanoparticles: Photocatalyst and Acetone Sensor. *Talanta,* **85,** 943-949.

[66] Faisal, M., Khan, S. B., Rahman, M. M., Jamal, A., Akhtar, K. and Abdullah, M. M., 2011. Role of Zno-Ceo2 Nanostructures as a Photo-Catalyst and Chemi-Sensor. *Journal of Materials Science & Technology,* **27,** 594-600.

[67] Faisal, M., Khan, S. B., Rahman, M. M., Jamal, A. and Abdullah, M. M., 2012. Fabrication of Zno Nanoparticles Based Sensitive Methanol

Sensor and Efficient Photocatalyst. *Applied Surface Science,* **258,** 7515-7522.

[68] Faisal, M., Khan, S. B., Rahman, M. M., Jamal, A., Asiri, A. M. and Abdullah, M. M., 2011. Smart Chemical Sensor and Active Photo-Catalyst for Environmental Pollutants. *Chemical Engineering Journal,* **173,** 178-184.

[69] Faisal, M., Khan, S. B., Rahman, M. M., Jamal, A., Asiri, A. M. and Abdullah, M. M., 2011. Synthesis, Characterizations, Photocatalytic and Sensing Studies of Zno Nanocapsules. *Applied Surface Science,* **258,** 672-677.

[70] Kos, T., Strissel, C., Yagci, Y., Nugay, T. and Nuyken, O., 2005. The Use of the Dpe Radical Polymerization Method for the Synthesis of Chromophore-Labelled Polymers and Block Copolymers. *European Polymer Journal,* **41,** 1265-1271.

[71] Temel, G., Aydogan, B., Arsu, N. and Yagci, Y., 2009. Synthesis of Block and Star Copolymers by Photoinduced Radical Coupling Process. *Journal of Polymer Science Part A: Polymer Chemistry,* **47,** 2938-2947.

[72] Dhiman, P., Chand, J., Kumar, A., Kotnala, R. K., Batoo, K. M. and Singh, M., 2013. Synthesis and Characterization of Novel Fe@Zno Nanosystem. *Journal of Alloys and Compounds,* **578,** 235-241.

[73] Zhang, D., Yang, J., Bao, S., Wu, Q. and Wang, Q., 2013. Semiconductor Nanoparticle-Based Hydrogels Prepared Via Self-Initiated Polymerization under Sunlight, Even Visible Light. *Scientific Reports,* **3,** No: 1399.

CURRICULUM VITAE

Name Surname:	Sajjad Dadashi Silab
Place and Date of Birth:	South Azerbaijan (Iran), 12 September1989
Address:	Department of Chemistry, Istanbul Technical University, 34469 Maslak, Istanbul, Turkey
E-Mail:	sajjad.silab@gmail.com
B.Sc.:	Amirkabir University of Technology, Tehran, Iran

PUBLICATIONS

- **Dadashi-Silab S.,** Asiri A. M., Khan S. B., Alamry K. A., and Yagci Y., Semiconductor nanoparticles for photoinitiation of free radical polymerization in aqueous and organic media. *Journal of Polymer Science Part A: Polymer Chemistry*, **2014**, 52, 1500-1507.
- **Dadashi-Silab S.,** Tasdelen M. A., Asiri A. M., Khan S. B., and Yagci Y., Photoinduced atom transfer radical polymerization using semiconductor nanoparticles. *Macromolecular Rapid Communications*, **2014**, 35, 454-459.
- **Dadashi-Silab S.,** Tasdelen M. A., Kiskan B., Wang X. C., Antonietti M., and Yagci Y., Photochemically mediated atom transfer radical polymerization using polymeric semiconductor mesoporous graphitic carbon nitride. *Macromolecular Chemistry and Physics*, **2014**, 215, 675-681.
- **Dadashi-Silab S.,** Bildirir H., Dawson R., Thomas A., and Yagci Y., Microporous thioxanthone polymers as heterogeneous photoinitiators for visible light induced free radical and cationic polymerizations. *Macromolecules*, **2014**, 47, 4607-4614.
- **Dadashi-Silab S.,** Tasdelen M. A., and Yagci Y., Photoinitiated atom transfer radical polymerization: Current status and future perspectives. *Journal of Polymer Science Part A: Polymer Chemistry*, **2014**, 52, 2878-2888.
- **Dadashi-Silab S.,** Kiskan B., Antonietti M., and Yagci Y., Mesoporous graphitic carbon nitride as a heterogeneous catalyst for photoinduced copper(I)-catalyzed azide-alkyne cycloaddition. *RSC Advances*, **2014**, 4, 52170-52173.

▪ **Dadashi-Silab S.**, Yar Y., Acar H. Y., and Yagci Y., Magnetic Iron Oxide Nanoparticles as Long Wavelength Photoinitiators for Free Radical Polymerization, *Polymer Chemistry*, **2015**, 6, 1918-1922

▪ Yetiskin O., **Dadashi-Silab S.**, Khan S. B., Asiri A. M., and Yagci Y., Visible light-induced copper(I)-catalyzed azide-alkyne cycloaddition with zinc oxide semiconductor nanoparticles, *Asian Journal of Organic Chemistry*, **2015**, 4, 442-444

▪ **Dadashi-Silab S.,** and Yagci Y., Copper(II) thioxanthone carboxylate as a photoswitchable catalyst for the photoinduced click chemistry, *Submitted*

▪ Taskin O. S., **Dadashi-Silab S.,** Jens W., Kiskan B., and Yagci Y., Highly Efficient and Reusable Microporous Schiff Base Network Polymer as Heterogeneous Catalyst for CuAAC Click Reaction, *In Press*

BOOK CHAPTERS

▪ Yagci Y., Tasdelen M. A., Kiskan B., Ciftci M., **Dadashi-Silab S.,** Taskin O. S., and Yilmaz G., Visible Light-induced Atom Transfer Radical Polymerization for Macromolecular Syntheses, *in Controlled Radical Polymerization, 248th ACS Symposium Series*

PRESENTATIONS

▪ Doran S, Murtezi E., **Dadashi-Silab S.**, Ciftci M., Yilmaz G., Tasdelen M. A., and Yagci Y., Photoinduced ATRP and CuAAC click reactions and their combinations for macromolecular syntheses, *249th ACS National Meeting*, Denver, CO, 2015 (*Oral presentation by Prof. Yagci*)

▪ **Dadashi-Silab S.**, Bildirir H., Dawson R., Thomas A., and Yagci Y., Microporous Thioxanthone Polymers as Heterogeneous Photoinitiators for Visible Light Induced Free Radical and Cationic Polymerizations, *5th EuCheMS Congress*, **2014**, Istanbul, Turkey *(Poster presentation)*

▪ **Dadashi-Silab S.**, Tasdelen M. A., Kiskan B., Wang X. C., Antonietti M., and Yagci Y., Photochemically Mediated Atom Transfer Radical Polymerization Using Polymeric Semiconductor Mesoporous Graphitic Carbon Nitride, *European Symposium on Photopolymer Science (ESPS 2014)*, Vienna, Austria (*Poster presentation*)

▪ Yagci Y., Tasdelen M. A., Kiskan B., Ciftci M., **Dadashi-Silab S.**, Visible light-induced atom transfer radical polymerization for macromolecular syntheses, *248th ACS National Meeting*, 2014, San Francisco, CA *(Oral presentation by Prof. Yagci)*

▪ **Dadashi-Silab S.,** Eslami H., Synthesis of Large Poly(methyl methacrylate) and Various Nonspherical Shaped Particles via Dispersion and Seeded Dispersion Polymerization, *10th International Seminar on Polymer Science and Technology (ISPST)*, **2012**, Tehran, Iran *(Oral presentation by Prof. Eslami)*